2 Sediment Erosion and Delivery from Toutle River Basin After the 1980 Eruption of Mount St. Helens: A 30-Year Perspective

Jon J. Major, Adam R. Mosbrucker, and Kurt R. Spicer

2.1 Introduction

Explosive volcanic eruptions can alter broad swaths of landscape by damaging or destroying vegetation, draping hillsides with volcanic ash, and filling valleys with volcanic sediment (e.g., Lipman and Mullineaux 1981; Sigurdsson et al. 1984; Newhall and Punongbayan 1996; Surono et al. 2012; Major and Lara 2013; Pierson and Major 2014). As a result, production and routing of runoff from rainfall and snowmelt can be greatly altered, erosional regimes modified, and fluxes of water and sediment greatly increased. In response to changes in water and sediment fluxes, geomorphic processes that modulate erosion, delivery, and storage of sediment can also change. Variations in geomorphic response and stability following volcanic eruptions in turn affect the nature and pace of ecological responses to eruptions (Dale et al. 2005a; Swanson and Major 2005).

Sediment-response trajectories after volcanic disturbance commonly exhibit a two-stage evolution (Gran et al. 2011) that is a function of topography. Explosive eruptions deposit fresh sediment in topographically diverse environments—on hillsides and in river valleys. The relative proportions of hillside and channel deposits vary with the nature of the eruption, basin orientation, and proximity to the volcano. Initial erosion of sediment from both hillsides and channels is typically very rapid and dramatic, which generates rates of sediment delivery that commonly are many tens to hundreds of times above typical pre-eruption levels (Pierson and Major 2014). Absent sediment recharge by frequent eruptions, this initial phase of response usually lasts only a few years before erosion and sediment delivery decline markedly. Commonly, only this immediate and acute phase of response affects catchments characterized predominantly by disturbed hillsides or those in which channels are relatively little disturbed. In such catchments, geomorphic processes usually return to those typical of pre-eruption conditions within a few years and sediment delivery swiftly returns to a level that is within the range of pre-eruption variation (e.g., Collins and Dunne 1986; Meyer and Martinson 1989; Major et al. 2000; Gran and Montgomery 2005; Yamakoshi et al. 2005). Although responses in such catchments commonly are immediate and short lived, some geomorphic responses and sediment delivery may be delayed or protracted owing to accumulation and rearrangement of large woody debris delivered to channels by an eruption (e.g., Lisle et al., Chap. 3, this volume), to landslides that may be more prevalent several years after an eruption (e.g., Swanson and Major 2005), or to releases of lakes created or enlarged by blockages of volcanic sediment (e.g., White et al. 1997). In contrast, rates and magnitudes of sediment release typically are greater and more prolonged from catchments in which valleys are thickly filled with volcanic sediment. In those catchments, initial geomorphic response and magnitude of sediment delivery owe largely to substantial incision and widening of channels as they adjust to altered flow regimes, changes in sediment character and supply, and changes in morphology (e.g., Janda et al. 1984; Manville 2002; Gran and Montgomery 2005; Pierson and Major 2014).

After channel forms and networks are reestablished, the most easily erodible sediment is depleted, and the hydraulic resistance of channels increases (e.g., Simon 1992), geomorphic response enters a second phase. In this response phase, sediment delivery is greatly diminished from peak levels but remains higher than pre-eruption levels because of persistent channel change. This phase of diminished, but still elevated, sediment delivery can persist for decades, perhaps centuries, depending on the magnitude of disturbance (Major 2004;

Glossary terms appear in ***bold italic face***.

J.J. Major (✉) • A.R. Mosbrucker • K.R. Spicer
U.S. Geological Survey, Cascades Volcano Observatory, 1300 SE Cardinal Court, Bldg 10, Suite 100, Vancouver, WA 98683, USA
e-mail: jjmajor@usgs.gov; amosbrucker@usgs.gov; krspicer@usgs.gov

C.M. Crisafulli, V.H. Dale (eds.), *Ecological Responses at Mount St. Helens: Revisited 35 years after the 1980 Eruption*,
https://doi.org/10.1007/978-1-4939-7451-1_2

Manville et al. 2009; Gran et al. 2011; Meadows 2014). In some instances, exceptional sediment delivery can be rejuvenated if lakes impounded by volcanic sediment breach and reinvigorate channel erosion (e.g., White et al. 1997; Manville et al. 2007).

Catchments affected by severe volcanic disturbance may never recover to pre-eruption geomorphic conditions—at least not over typical human timeframes. Instead, they may attain a degree of stability and ecological function under different equilibrium conditions (e.g., Gran and Montgomery 2005; O'Connor et al. 2013; Pierson and Major 2014), and this can have prolonged societal consequences. Here, we provide a multi-decade perspective of the hydrologic and geomorphic (hydrogeomorphic) responses of Toutle River basin at Mount St. Helens in the context of the two-stage conceptual-response framework. Toutle River basin, which drains the volcano's north and west flanks as well as terrain to the north of the mountain, was affected by the most diverse and severe disturbances caused by the 18 May 1980 eruption. As a result, its catchments have shown the most varied and prolonged hydrogeomorphic responses.

The 18 May 1980 eruption of Mount St. Helens consisted of an ensemble of volcanic processes (Fig. 2.1) that dramatically altered landscapes and ecosystems of several catchments surrounding the volcano (Lipman and Mullineaux 1981; Dale et al. 2005b). That ensemble—a rockslide–***debris avalanche***; a laterally directed ***pyroclastic density current*** (PDC), commonly called the lateral blast, but herein called the ***blast PDC***; ***lahars*** (volcanic debris flows); ***pyroclastic flows***; and fall of volcanic ash (***tephrafall***)—caused gradients of landscape disturbances (e.g., Lipman and Mullineaux 1981; Swanson and Major 2005; Lisle et al., Chap. 3, this volume) which affected the fluxes of water and sediment through catchments to varying degrees and for substantially different durations (Major et al. 2000; Major and Mark 2006).

The nature and duration of hydrogeomorphic responses at Mount St. Helens reflect the nature and severity of landscape disturbance. In some catchments, such as Green River and Clearwater Creek (Fig. 2.1), hydrogeomorphic responses were modest and short-lived, even though large proportions of their areas were affected, because only hillsides were disturbed by the primary events (Collins and Dunne 1986; Meyer and Martinson 1989; Lisle et al., Chap. 3, this volume). Fluxes of water and sediment in those catchments returned to typical pre-eruption levels within a few years (Major et al. 2000; Major and Mark 2006; Lisle et al., Chap. 3, this volume). In other catchments where the eruption buried substantial proportions of valley bottoms with thick volcanic deposits, such as North Fork Toutle River (Fig. 2.1), hydrogeomorphic responses were of greater magnitude and have been much longer lived. In those catchments, the greatest magnitudes of channel change occurred in the first few years after the eruption, when channels were furthest out of equilibrium (e.g., Rosenfeld and Beach 1983; Martinson et al. 1984; Meyer et al. 1986; Meyer and Martinson 1989; Simon 1999; Zheng et al. 2014). After an initial adjustment period, both the magnitudes and rates of channel changes in those catchments slowed considerably (Martinson et al. 1986; Meyer and Dodge 1988; Simon 1999; Hardison 2000; Zheng et al. 2014), and consequent sediment delivery declined sharply (Major et al. 2000). In North Fork Toutle River catchment, however, sediment fluxes remain significantly above pre-eruption levels even after more than 30 years since the eruption.

In this chapter, we summarize erosion and long-term sediment delivery from Toutle River basin. We examine some of the underlying causes for its persistently high sediment fluxes, particularly from North Fork Toutle River catchment. We first provide a synopsis of the disturbances caused by the cataclysmic 1980 eruption and their hydrogeomorphic impacts. We then present an update of the suspended-sediment flux from Toutle River basin. Analyses of volumetric change in erosion and deposition along upper North Fork Toutle River valley during the second and third decades after eruption follow. We use analyses of volumetric change and patterns of erosion to consider why sediment flux from upper North Fork Toutle River has remained so persistently elevated.

2.2 Volcanic Disturbance Processes and Deposits in Toutle River Basin

Toutle River basin was affected by four major volcanic processes (Fig. 2.1): a rockslide–debris avalanche, a blast PDC and associated rain of fine ash (particles ≤0.25 mm) from its turbulent cloud, large lahars, and pyroclastic flows. Detailed discussions and summaries of these processes and the sequencing of processes on 18 May are given in Lipman and Mullineaux (1981), Criswell (1987), Fairchild (1987), Scott (1988), Glicken (1996), Swanson and Major (2005), Belousov et al. (2007), Esposti Ongaro et al. (2012), and Waitt (2015).

The rockslide–debris avalanche resulting from collapse of the volcano's north flank buried upper North Fork Toutle River valley. It filled about 60 km^2 of valley with 2.5 km^3 of mostly gravelly sand to an average depth of 45 m. Locally, the deposit is as thick as 200 m (Voight et al. 1981). The debris avalanche obliterated mature forest on the valley floor and slammed against Johnston Ridge opposite the volcano. Although most of it turned and flowed down the valley after hitting Johnston Ridge, part of it surged through Spirit Lake, and part crossed Johnston Ridge and flowed down South Coldwater Creek valley before rejoining North Fork Toutle River valley (Figs. 2.2 and 2.3). Its deposit blocked several

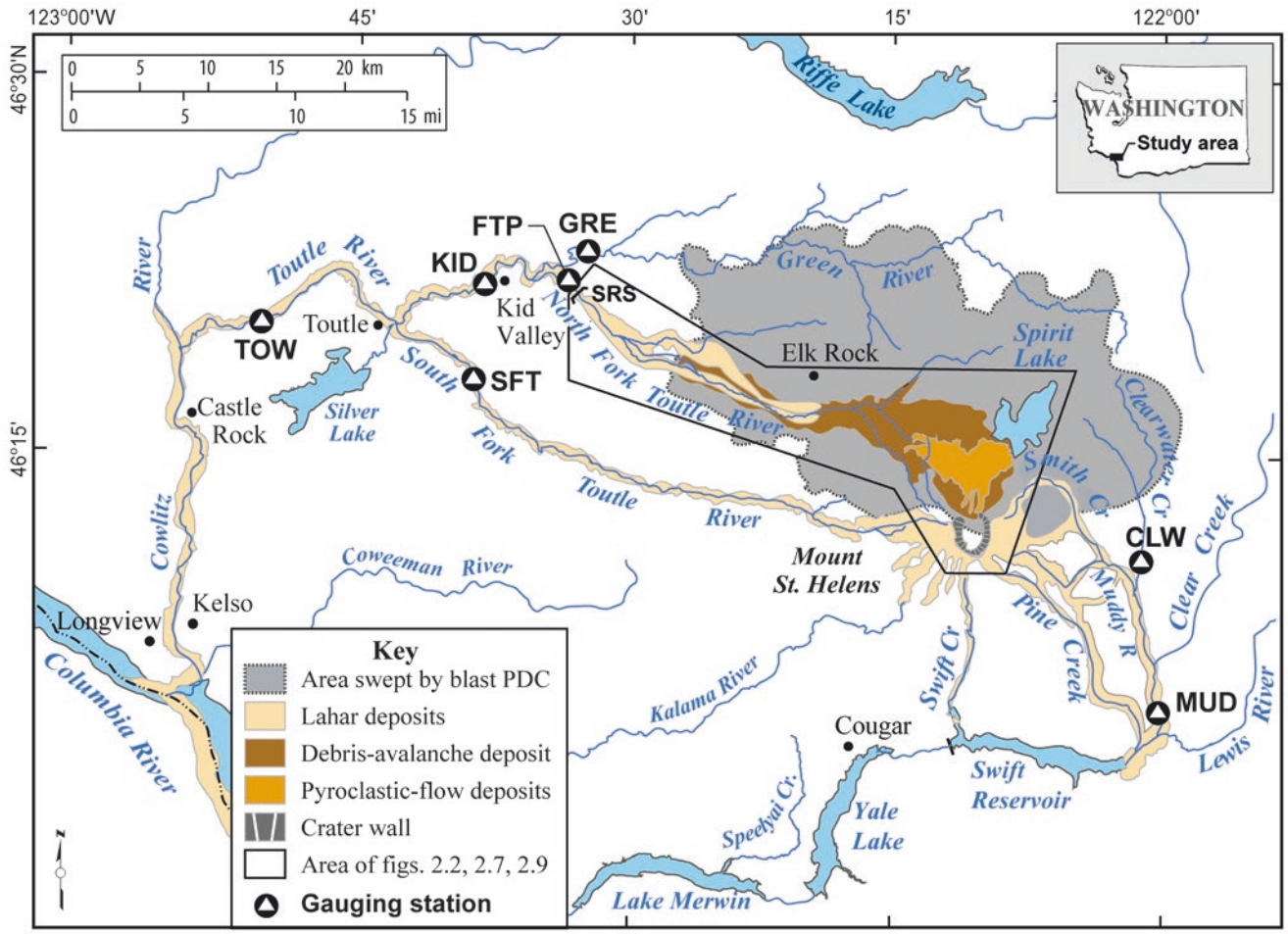

Fig. 2.1 Distribution of volcanic disturbance zones of 1980 Mount St. Helens eruption and locations of gauging stations. *SRS* sediment-retention structure. Gauging stations: *GRE* Green River, *FTP* additional North Fork Toutle River station, *KID* Kid Valley on North Fork Toutle River, *SFT* South Fork Toutle River, *TOW* lower Toutle River, *CLW* Clearwater Creek, *MUD* Muddy River. (Modified from Major et al. 2000).

tributary channels and impounded new lakes of varying size. Several small lakes breached their impoundments within weeks to months (Janda et al. 1984; Simon 1999). The two largest new lakes (Castle and Coldwater) still retain substantial volumes of water (20 and 90 million m^3, respectively) behind impoundments having reinforced outlets (Figs. 2.2 and 2.3). Spirit Lake was displaced upward and its outlet buried. To prevent catastrophic breaching of the blockage, water was pumped temporarily from the lake over the blockage crest and onto a stable part of the deposit, forming Truman channel (Paine et al. 1987; see Fig. 2.2), while an outlet tunnel was bored through bedrock (Fig. 2.2). Since 1985, water from Spirit Lake has drained westward through the tunnel into South Coldwater Creek and eventually back to North Fork Toutle River.

Failure of the volcano's north flank unroofed magma that had intruded high into the edifice and unleashed a violent, laterally directed, gas-charged explosion (Hoblitt et al. 1981; Waitt 1981; Voight 1981). That explosion triggered a widespread, rapidly moving, hot PDC—the blast PDC—that swept across 570 km^2 of rugged landscape to the north and removed, toppled, or scorched mature forest. The blast PDC deposited as much as 1.5 m of graded gravel to fine sand capped by as much as 6 cm of fine silt (Hoblitt et al. 1981; Waitt 1981). Within about 10 km of the volcano, the blast PDC stripped the landscape of soil and vegetation; from there to its distal limits (20 km north and about 30 km east to west extent), it toppled mature forest (Moore and Sisson 1981; Swanson and Major 2005). The zone of toppled trees is fringed by standing, scorched forest (Winner and Casadevall 1981). In Green River catchment (Fig. 2.1), the blast PDC was the only volcanic disturbance process.

Rapid melting of snowpack by the blast PDC in the headwaters of South Fork Toutle River catchment on the volcano's west flank and dewatering of debris-avalanche deposit in North Fork Toutle River valley triggered two large (14–140 million m^3) lahars in Toutle River basin on 18 May (Janda et al. 1981; Fairchild 1987; Scott 1988; Waitt 1989).

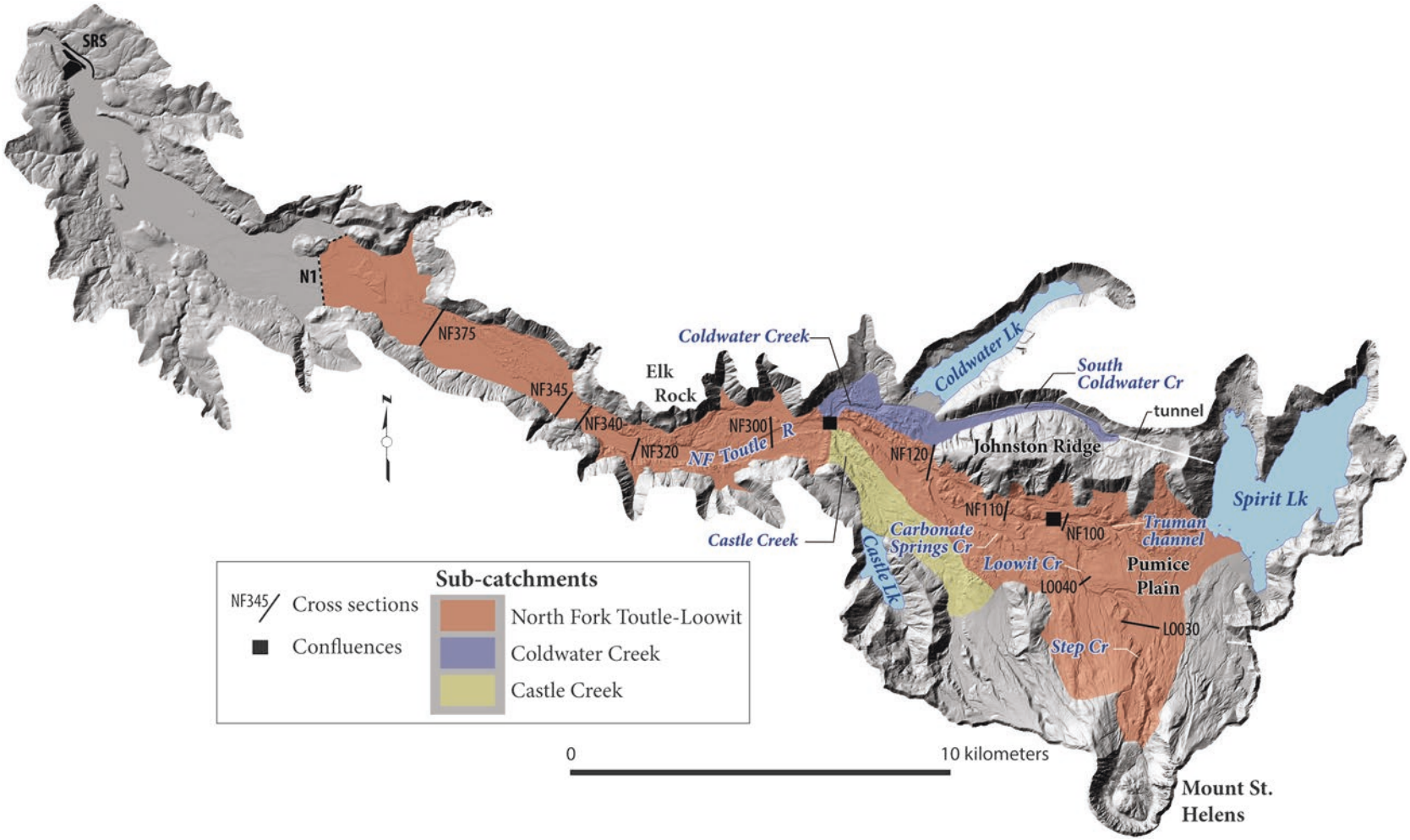

Fig. 2.2 Shaded-relief digital elevation model of upper North Fork Toutle River catchment showing 2009 topography (Mosbrucker 2014), locations cited in text, and select cross sections of channel geometry surveys (e.g., NF320). *Red* shading shows approximate upper North Fork Toutle–Loowit channel sub-catchment in which decadal-scale volumes of erosion and deposition across debris-avalanche deposit were estimated (outlined downstream only to site of former N1 retention structure); *yellow* shading shows Castle Creek sub-catchment; *blue* shading shows Coldwater Creek sub-catchment. Major channels across the debris-avalanche deposit are labeled. *Black boxes* mark confluences of North Fork Toutle River, Castle Creek, and Coldwater Creek (west) and North Fork Toutle River, Truman channel, and Loowit Creek (east). These confluences, and cross sections NF340 and LO030, denote reach boundaries shown in Table 2.1. *SRS* is the sediment-retention structure.

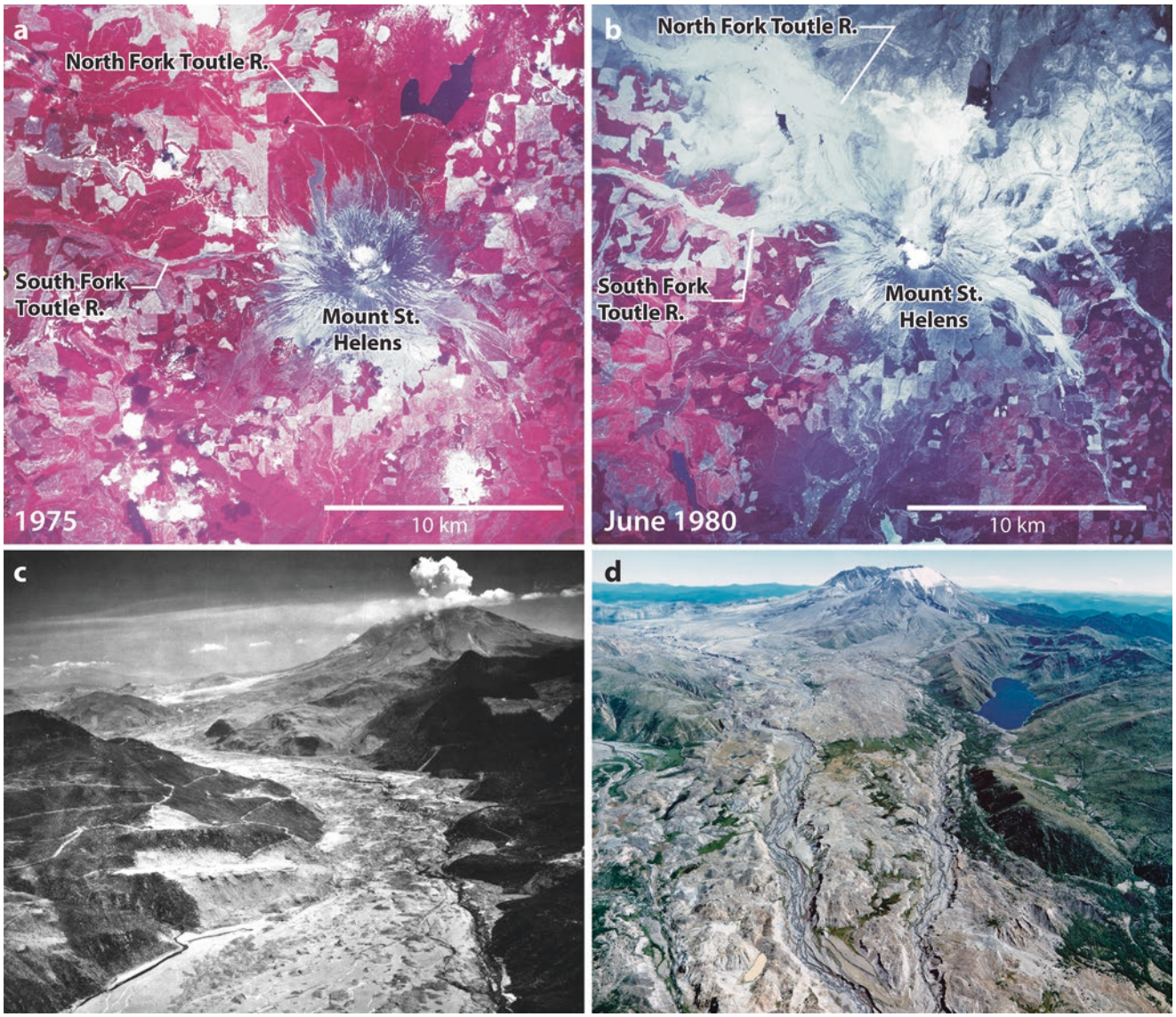

Fig. 2.3 Images of volcanic impact and erosion in upper North Fork Toutle River valley. **a**, **b** are high-altitude (false-color infrared) vertical aerial photographs of Mount St. Helens taken in 1975 and on 19 June 1980, respectively. Spirit Lake is in the *upper right* quadrant of each image. Compare zones of volcanic impact in (**b**) with disturbance zones in Fig. 2.1. **c** Oblique aerial photograph of debris-avalanche deposit in upper North Fork Toutle River valley. Valley constriction is the Elk Rock reach shown in Fig. 2.2. USGS photograph by A. Post and R.M. Krimmel, 30 June 1980. **d** Oblique aerial photograph of upper North Fork Toutle River valley showing erosion of debris-avalanche deposit. Castle Lake is in the *upper right* quadrant of photograph; lower edge of South Coldwater Creek valley is in the *left center* of photograph. (Image courtesy of Washington State Department of Transportation approximately 1993).

The smaller, flash-flood-like South Fork Toutle River lahar deposited gravelly sand across valley floor and floodplain, ranging in thickness from a few centimeters on the volcano's flank to a few meters farther downstream (Janda et al. 1981; Scott 1988; Waitt 1989). The North Fork Toutle River lahar was a much larger, longer-lasting event that started later in the day. Its exceptional volume (140 million m^3 just downstream of the debris-avalanche deposit and 120 million m^3 at the mouth of Toutle River, 70 km from source), minimal attenuation, and long duration (11 h at the mouth of Toutle River) damaged houses, lumber facilities, and infrastructure along the North Fork Toutle, Toutle, and Cowlitz River valleys (Janda et al. 1981; Fairchild 1987). The North Fork Toutle River lahar deposited meters-thick gravelly to muddy sand along the channel bed, valley floor, and floodplain, especially in lower Toutle, Cowlitz, and Columbia Rivers (e.g., Lombard et al. 1981; Schuster 1981).

Within tens of minutes of the debris avalanche and blast PDC, a sustained vertical eruption column rose more than 20 km (Christiansen and Peterson 1981). Ash (particles ≤2 mm) from that eruption column drifted downwind and deposited tephrafall over tens of thousands of square kilometers

(Sarna-Wojcicki et al. 1981). This eruptive phase lasted for more than 9 h. During that time, partial collapses of the eruption column generated pumiceous pyroclastic flows that rushed from the new crater and deposited sheets of ash and pumice lapilli (particles 2–64 mm) atop the debris-avalanche deposit in the area now known as the Pumice Plain (Criswell 1987; Brand et al. 2014; Figs. 2.1 and 2.2). Five subsequent eruptions in summer 1980 also produced pumiceous pyroclastic flows that added to the fill atop the debris-avalanche deposit (Rowley et al. 1981). Deposits from these flows cover about 15 km^2; thicknesses of individual flow units range from 0.25 to 10 m, and the collective deposit thickness from the succession of flows is as much as 40 m (Rowley et al. 1981).

2.3 Hydrogeomorphic Impacts of the 1980 Eruptions in Toutle River Basin

Landscape changes caused by the cataclysmic eruption of Mount St. Helens profoundly altered landscape hydrology and geomorphology. Volcanic processes damaged or destroyed mature forest over hundreds of square kilometers, draped hillsides with sediment having a nearly impervious surface, and filled or altered the character of major channels draining the volcano (Fig. 2.3). Later eruptions in summer 1980 added to, but did not cause additional, landscape disturbances. Aside from upper North Fork Toutle River and South Coldwater Creek valleys, which were deeply buried by debris-avalanche deposit, sediment deposition caused little change to fundamental pre-eruption landforms. Even so, prevailing geomorphic processes were altered. Because disturbances caused by the 1980 eruptions occurred before the onset of the wet season, they can be considered as a single event with regard to post-eruption hydrogeomorphic response. Therefore, in the following discussions, we refer to them in aggregate as the 1980 eruption.

2.3.1 Hillsides

Forested Cascade Range hillsides typically have permeable, organic-rich soils showered by low- to moderate-intensity rainfall (14–30 mm h^{-1}; Miller et al. 1973; see also Western Regional Climate Center 2015). As a result, infiltration capacities are high, about 75–100 mm h^{-1} or more (Johnson and Beschta 1980; Leavesley et al. 1989; McGuire et al. 2005), and flow moves through the landscape largely in the subsurface (Jones 2000; McDonnell 2003; McGuire et al. 2005). Consequently, annual sediment yields are low, a few hundred tonnes (t) km^{-2} (e.g., Major et al. 2000; Roering et al. 2010; Czuba et al. 2011).

At Mount St. Helens, forest damage and deposition of fine ash in 1980 altered fluxes of water from hillsides to channels. Destruction of a broad swath of forest significantly reduced foliar interception and altered seasonal evapotranspiration. Loss of foliar interception allowed more precipitation to reach the ground surface, and changes in evapotranspiration kept soils wetter than usual. Deposition of fine ash markedly reduced the infiltration of rainfall and snowmelt across the landscape near Mount St. Helens. Rainfall experiments conducted in summer 1980 on hillsides affected by the blast PDC showed spatially averaged infiltration capacities had been reduced to as little as 2 mm h^{-1} (Leavesley et al. 1989), and they remained <10 mm h^{-1} 1 year later (Swanson et al. 1983; Leavesley et al. 1989). After nearly 20 years, plot-specific infiltration capacities remained three to five times lower than pre-eruption capacities (Major and Yamakoshi 2005). Loss of foliar interception, changes in evapotranspiration, and reduction of surface infiltration changed the mode of water transfer through the hydrological system from one dominated by subsurface flow to one dominated by overland flow (Leavesley et al. 1989; Pierson and Major 2014). The dominance of overland flow persisted for more than 1 year, and even after 20 years high-intensity (>25 mm h^{-1}) rainstorms remained capable of triggering overland flow (Major and Yamakoshi 2005).

This fundamental change in hillside hydrology altered sediment erosion and transport processes. Hillside erosion and transport in the pre-eruption landscape were dominated by tree throw, bioturbation, soil creep, and mass wasting (e.g., Gabet et al. 2003; Roering et al. 2010). Dominance of overland flow after the 1980 eruption triggered extensive slope erosion through development of rill and gully networks across ash-covered slopes (Swanson et al. 1983; Collins and Dunne 1986).

2.3.2 Channels

Channel changes caused by the eruption had variable hydrological ramifications. The channels of South Fork Toutle, lower North Fork Toutle, and Toutle Rivers were straightened and smoothed and changed from gravel-bedded, pool-riffle systems to simplified sand-bedded corridors stripped of riparian vegetation (Janda et al. 1984). These changes enhanced the hydraulic efficiency of channels (Major and Mark 2006; Pierson and Major 2014). In contrast, deposition of the debris avalanche in upper North Fork Toutle River valley hydrologically disconnected the upper valley from the lower, which temporarily reduced water delivery downstream. The debris-avalanche deposit blocked tributary channels, and its irregular surface, formed of mounds and closed depressions, disrupted through-going flow. Drainage devel-

opment across the debris-avalanche deposit began on the afternoon of 18 May when springs poured forth from melting ice and trapped groundwater, and ponds that formed in depressions filled and breached. Sediment entrained during this dewatering and breaching process across the debris-avalanche deposit eventually generated the North Fork Toutle River lahar (Janda et al. 1981, 1984). Breakouts of small lakes impounded at mouths of tributary channels, controlled releases of water from the largest impounded lakes, pumping of water from Spirit Lake across the deposit surface during tunnel construction, subsequent meltwater lahars and floods in later eruptions (e.g., Waitt et al. 1983), and rainfall runoff augmented drainage development. It took nearly 3 years to fully integrate a new drainage network across the deposit surface (Rosenfeld and Beach 1983; Meyer 1995; Simon 1999).

These hydrological changes resulted in discharge peaks in Toutle River basin that were larger than pre-eruption peaks for a given amount of rainfall (Major and Mark 2006). Hydrological responses were greater in the South Fork Toutle River and North Fork Toutle River catchments, subject to both hillside and channel disturbances, than in the Green River catchment, subject only to hillside disturbance. Peak flows generated by runoff from autumn storms increased tens of percent along all major channels of Toutle River basin through 1984 and increased to a lesser extent, as measured along lower Toutle River, from 1985 to 1989. Pre- and post-eruption peak discharges are statistically indistinguishable after 1989.

Channel-network development across the debris-avalanche deposit, in conjunction with increased transport capacity, triggered substantial erosion and sediment transport (Janda et al. 1984; Dinehart 1998; Simon 1999; Major 2004). Even low- to moderate-magnitude flows (discharges ≤2-year flood) transported large quantities of sediment (Major 2004). Repeat surveys of an extensive network of channel cross sections in Toutle River basin show the greatest channel changes were on North Fork Toutle River where it crossed the debris-avalanche deposit (Meyer and Martinson 1989). There, early channel changes commonly followed a multistage evolutionary process (Meyer and Martinson 1989): (1) channel initiation, (2) incision, (3) aggradation and widening, and (4) episodic scour and aggradation with little net change in bed elevation. Persistent and progressive incision and widening dominated channel development upstream of a valley constriction at Elk Rock (upstream of NF320; Figs. 2.2 and 2.4). Downstream of that valley constriction, aggradation and widening dominated until the mid-1980s, after which secondary incision accompanied continued widening (Fig. 2.4). North Fork Toutle River channel and those of its headwater tributaries incised by tens of meters and widened by hundreds of meters upstream of Elk Rock (e.g., NF100, NF300; Fig. 2.4). Downstream, the channel aggraded as much as 15 m and widened by hundreds of meters (e.g., NF345; Fig. 2.4). The greatest and most rapid channel changes occurred within the first few years after the 1980 eruption, but the principal channel and its main tributaries were subject to progressive, long-term geometric adjustments (Fig. 2.4).

Channel gradient affected initial changes of South Fork Toutle River channel as well as lahar-affected channels east of the volcano (Meyer and Martinson 1989; Hardison 2000). In steep upstream reaches, lahar-affected channels generally incised by several meters and widened by a few tens of meters during the first year following eruption but then aggraded by a few meters and underwent episodic scour and aggradation in subsequent years. In contrast, shallow-gradient reaches downstream aggraded by a few meters and widened by a few tens of meters during the first year after eruption and then incised by a few meters in following years. Similar to channel changes across the debris-avalanche deposit, those in lahar-affected channels were most rapid during the first few years after the eruption.

In Green River catchment, affected only by the blast PDC, the channel aggraded by as much as a meter during the first few winter storms following the 1980 eruption as sediment flushed from hillsides accumulated. However, during later storms that same winter, the channel incised (Meyer and Martinson 1989). Subsequently, little except local channel change occurred. Widening of Green River channel, as well as of channels in other catchments affected only by the blast PDC (e.g., Clearwater Creek; Fig. 2.1), was generally constrained by riparian vegetation that rapidly resprouted and maintained bank cohesion and was strongly influenced by large woody debris toppled into the channel by the PDC (Lisle 1995; Lisle et al., Chap. 3, this volume).

Approximately 5 years after the 1980 eruption, rates and magnitudes of geometric changes in channels affected by lahars and those in catchments affected by the blast PDC had largely diminished (Meyer and Martinson 1989; Simon 1999; Hardison 2000; Lisle et al., Chap. 3, this volume). By then, relatively minor changes in bed elevations and channel widths were likely within the range of variations characteristic of pre-eruption conditions, especially in catchments affected only by the blast PDC. It is worth noting, however, that regional climate was relatively dry during the decade following the eruption and few large floods occurred (Major 2004; Swanson and Major 2005). Large storm events in the 1990s and 2000s generated a few larger floods (20-year to ~100-year return interval flows), which caused channel changes that not only exceeded the likely range of pre-eruption variations, but in some channels caused changes that exceeded those documented during the first decade after the eruption (Simon 1999; Lisle et al., Chap. 3, this volume; Mosbrucker et al. 2015).

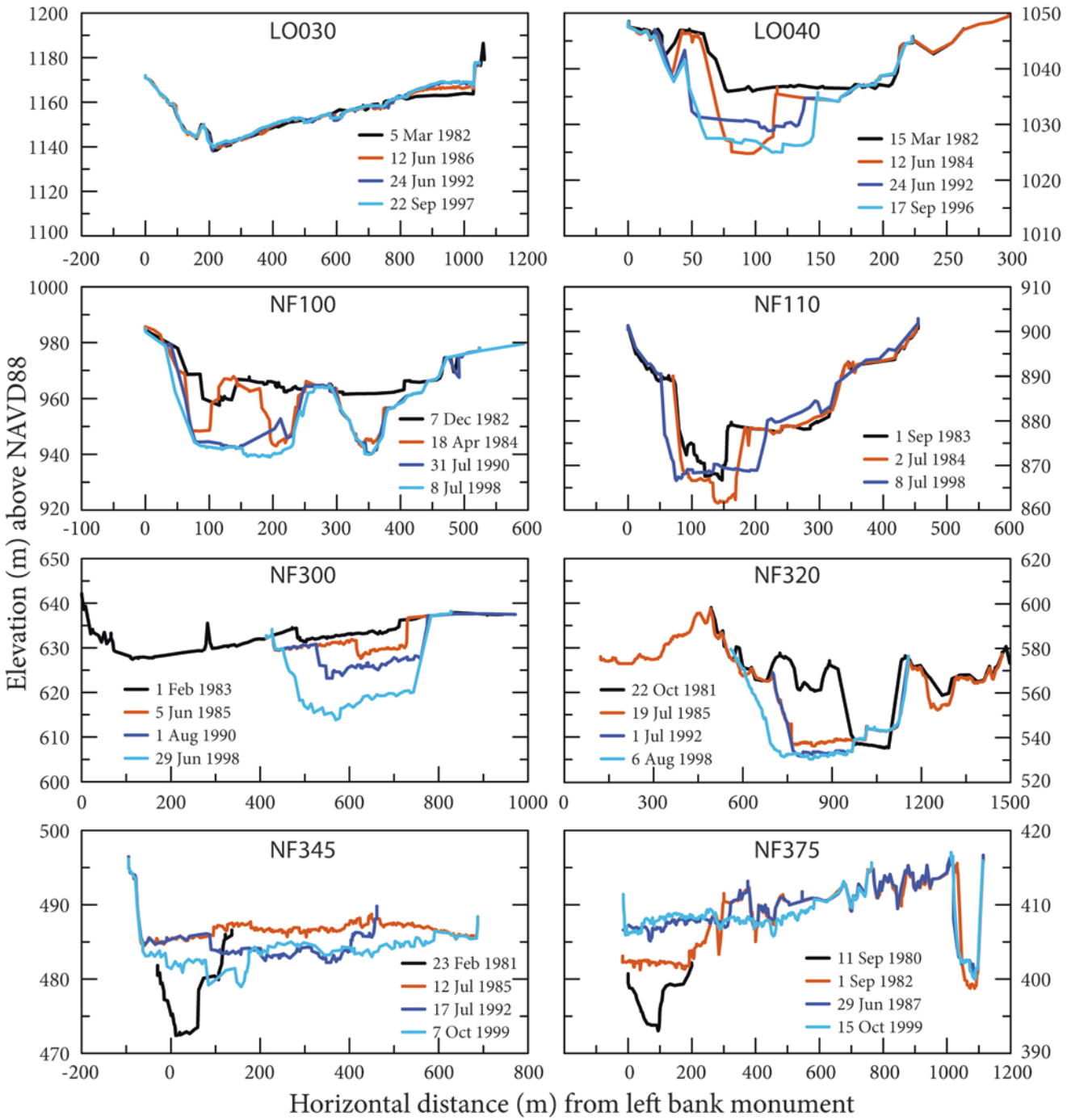

Fig. 2.4 Cross-section profiles from select locations on debris-avalanche deposit from 1980 to 1999. (See Figs. 2.2 and 2.7 for section locations).

2.4 Long-Term Sediment Transport from Toutle River Basin

Post-eruption sediment redistribution at Mount St. Helens is mostly by fluvial transport (Major 2004). The dominance of post-eruption fluvial transport contrasts with predominant lahar transport at many other volcanoes, especially those in tropical climates (Pierson and Major 2014). The scarcity of post-1980 lahars at Mount St. Helens is largely a consequence of the region's low to moderate rainfall intensities. However, it also reflects engineering measures undertaken to prevent catastrophic breaching of impounded lakes (Willingham 2005) and the general character of post-1980 eruptions at the volcano—quiescent dome building rather

than violent explosions. The few explosions and minor dome collapses that occurred while the volcano was clad in snow triggered the most notable post-1980 lahars (e.g., Waitt et al. 1983; Pringle and Cameron 1999).

Gauging stations operating at the time of or established after the 1980 eruption provide measures of discharges of water and suspended sediment. Stations in Toutle River basin (Fig. 2.1) are located downstream of the debris-avalanche deposit (KID on lower North Fork Toutle River; TOW[1] on lower Toutle River), along a lahar-affected channel (SFT on lower South Fork Toutle River), and in a basin affected solely by the blast PDC (GRE on Green River). KID measured combined discharges from the North Fork Toutle and Green River catchments, and TOW integrates discharges from the entire Toutle River basin. All four stations operated continuously from 1982 to 1994; KID and GRE were decommissioned in 1994, and SFT was decommissioned in 2014. As of 2015, TOW remained in operation. An additional station (FTP) was established on North Fork Toutle River just above the Green River confluence and has measured water discharge intermittently since 1990 and suspended-sediment discharge intermittently since 2001.

Suspended-sediment transport in Toutle River basin increased significantly following the 1980 eruption (Figs. 2.5 and 2.6). The magnitude and duration of excessive sediment loads vary as a function of the type of volcanic disturbance. Elevated levels of suspended sediment have been greatest and of longest duration from upper North Fork Toutle River catchment, buried deeply by debris-avalanche deposit (Dinehart 1998; Major et al. 2000; Major 2004). By contrast, elevated levels of suspended sediment were least and of shortest duration from Green River catchment, deforested and draped with tephra by the blast PDC. Fluctuations in annual loads (Fig. 2.5) owe mainly to variations in annual climate and infrequent, high-discharge floods.

Normalized suspended-sediment yields (load normalized by upstream basin area) measured at KID and TOW were initially several hundred times greater than probable pre-eruption yields (Fig. 2.6). Those high yields, caused mainly by sediment flushed from hillsides in Green River catchment and from channels eroded on the debris-avalanche deposit, declined sharply over the first 5 years following the 1980 eruption. They declined further in the late 1980s following construction by the US Army Corps of Engineers of a large sediment-retention structure (SRS) on North Fork Toutle River above the Green River confluence (Willingham 2005) (Fig. 2.1). Despite the decline from peak yields in the early 1980s, yield from the debris-avalanche deposit (measured below the SRS) continues at a level ~10–50 times greater than probable pre-eruption level even after more than 30 years (Fig. 2.6). By contrast, yield from Green River catchment was initially 100 times less than that from North Fork Toutle River catchment and only about 10 times greater than probable pre-eruption level (Fig. 2.6). Initially high rates were caused by development of rills and gullies on hillsides. Because erosion of tephra from hillsides stabilized quickly (Swanson et al. 1983; Collins and Dunne 1986), sediment yield from Green River catchment declined rapidly and returned to pre-eruption level within about 5 years (Fig. 2.6). Yield from South Fork Toutle River, a catchment affected mainly by a large lahar, was initially about 20 times greater than probable pre-eruption level (Fig. 2.6) as both newly deposited and centuries-old sediment were scoured from the system. But it also decreased sharply in the first few years after the eruption once the most easily entrained sediment was evacuated. However, sediment flux from South Fork Toutle River catchment subsequently fluctuated considerably (Fig. 2.5), with loads in the 1990s and 2000s sometimes equaling those of the mid-1980s. Although its yield may still be above probable pre-eruption level (Fig. 2.6), since 2000, its average yield has been within the range of variation of rivers in the western Cascade Range.

Substantial post-eruption sediment transport and resultant channel aggradation are common around Cascade Range volcanoes. Thick, post-eruptive alluvial fills have been described along other channels draining Mount St. Helens (Crandell 1987; Major and Scott 1988) as well as along channels draining Mount Hood (Pierson et al. 2011), Mount Rainier (Zehfuss et al. 2003), Mount Baker (Pringle and Scott 2001), and Glacier Peak (Beget 1982). Persistent sediment release from the Mount St. Helens debris-avalanche deposit has caused significant socioeconomic impact (Willingham 2005) and continues to present mitigation challenges. But why has such elevated sediment release persisted, and what are the predominant sediment sources? In Sect. 5, we address these questions by analyzing topographic changes among repeated collections of topographic data.

2.5 Topographic Change Across the Debris-Avalanche Deposit from 1987 to 2009: DEM Analyses

With the exception of Green River catchment, high sediment yields from Toutle River basin were caused mainly by post-eruption channel erosion rather than by hillside erosion. Both within and among disturbance zones, rates and

[1]Prior to 1980, the station measuring discharge on Toutle River was located near Silver Lake, but that station was destroyed by the North Fork Toutle lahar. A temporary station (THW) was established 9 km downstream of the location of station TOW (Fig. 2.1) shortly after the eruption. Station TOW was established in March 1981. THW and TOW operated simultaneously until the end of water year 1982. Because there are no significant tributaries that enter Toutle River between TOW and THW, their records are combined to provide the sediment discharge for water year 1981 (see Dinehart 1998).

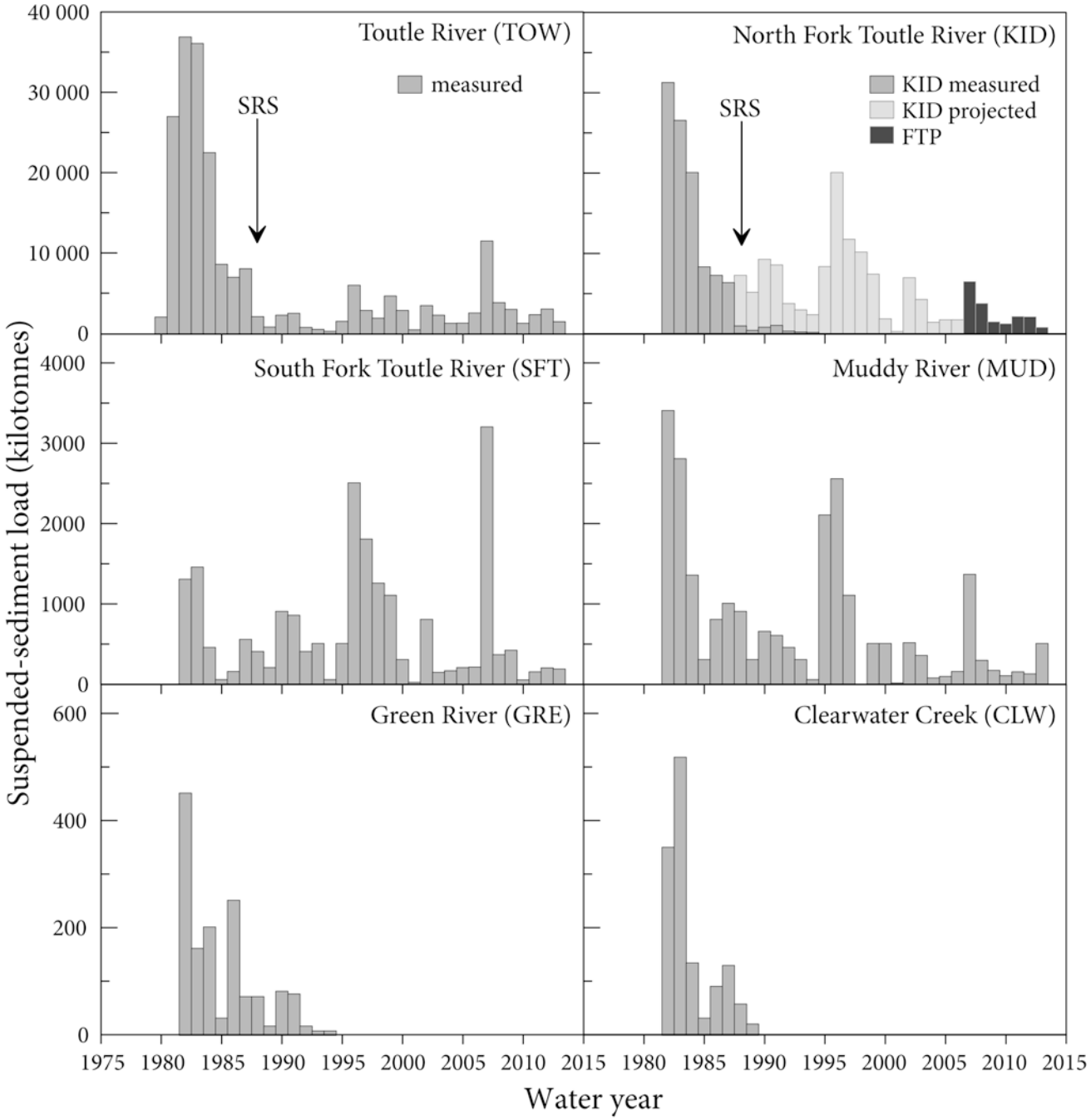

Fig. 2.5 Time series of suspended-sediment loads measured at various gauging stations at Mount St. Helens. The *lightest* colored bars for North Fork Toutle River show projected load that would have been measured if the sediment-retention structure (SRS) had not been constructed; the *darkest* bars show loads measured at station FTP just downstream of the SRS. Note the approximately order-of-magnitude change in vertical scale for different disturbance zones. See Fig. 2.1 for basin disturbance and gauging station locations. (Modified from Major 2004).

magnitudes of channel changes and degrees of channel stabilization varied greatly. Changes in rates and magnitudes of sediment discharge from catchments of Toutle River basin can be tied closely with changes in rates and magnitudes of channel and hillslope erosion. For example, the relative magnitudes and swift decline of sediment yield from Green River catchment compared with other catchments in the basin (Major et al. 2000) can be tied to modest deposit thicknesses and rapid stabilization of rills and gullies on hillsides in the catchment (Collins and Dunne 1986). Measurements of sediment discharge among basin catchments show clearly that the primary source of persistently elevated sediment delivery

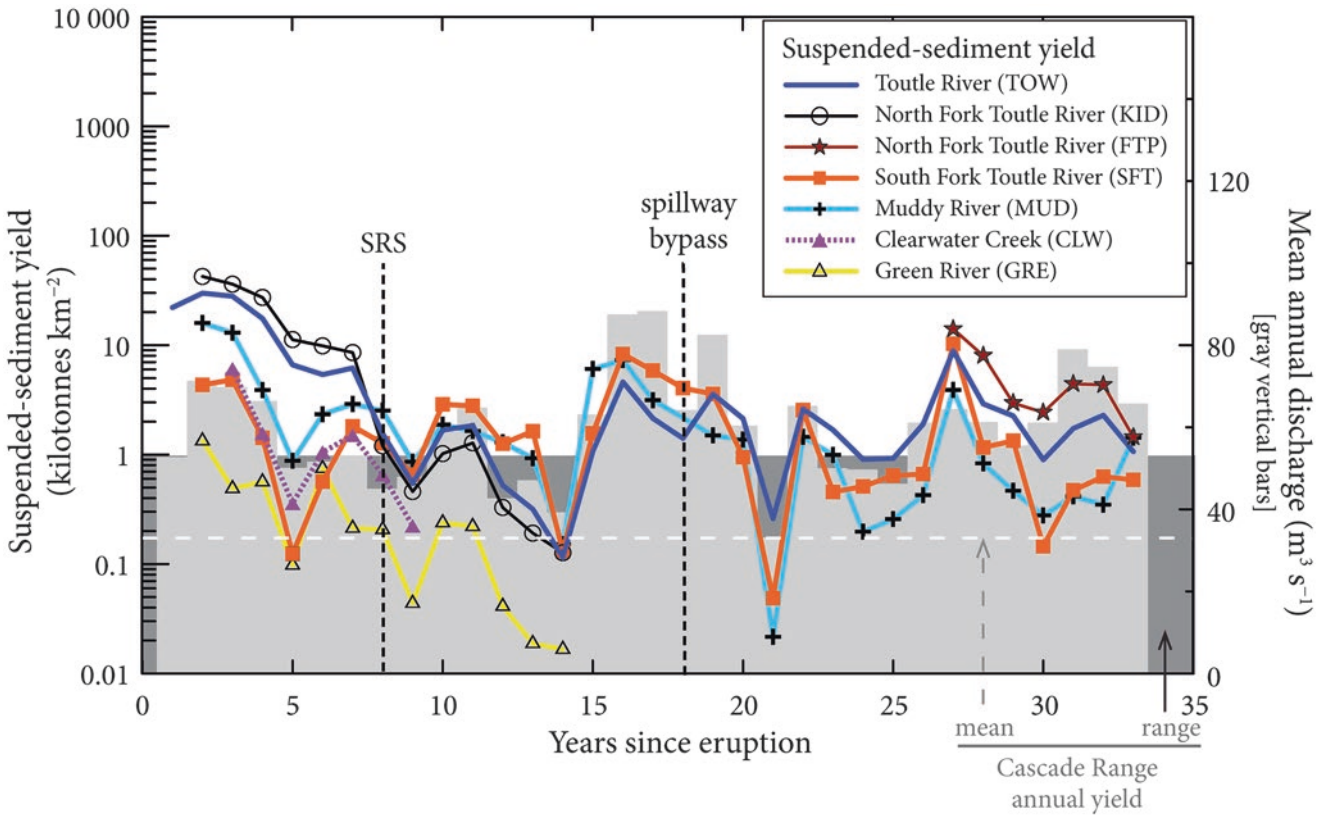

Fig. 2.6 Time series of suspended-sediment specific yields (load per unit basin area) at Mount St. Helens. See Fig. 2.1 for basin disturbances and gauge locations. *Background shaded region* depicts range and *dashed horizontal line* depicts approximate mean value of mean annual yields of several Cascade Range rivers. *Vertical bars* show mean annual discharge measured at TOW on Toutle River. *SRS line* marks completion date of the sediment-retention structure on North Fork Toutle River in water year 1988. *Spillway bypass line* indicates when water and sediment began passing over the SRS spillway in 1998. (Modified from Major et al. 2000).

is the debris-avalanche deposit in upper North Fork Toutle River valley. Here we examine spatial patterns of erosion and deposition across the debris-avalanche deposit during two time periods that follow the initial peak and sharp decline of sediment delivery from upper North Fork Toutle valley: (1) the approximate decade from 1987 to 1999 and (2) the decade from 1999 to 2009. These decadal periods are bracketed by digital elevation models (DEMs) that can be used to produce derivative models showing topographic change across the deposit. These broad snapshots of spatial change provide a more holistic view of evolving patterns of geomorphic change across the deposit than can be obtained from periodic resurveys of spatially discrete channel cross sections. We use these decadal-scale holistic views of patterns of geomorphic change to elucidate sources and causes of persistently elevated levels of sediment delivery from upper North Fork Toutle valley.

Channel cross-section surveys on the debris-avalanche deposit (e.g., Fig. 2.4) show rates and magnitudes of change in channel-bed elevation have diminished greatly since the mid-1980s (Meyer and Martinson 1989; Simon 1999; Zheng et al. 2014). Persistently elevated sediment delivery despite these diminished changes in channel-bed elevation implies that lateral channel adjustment is the principal cause of ongoing fluvial instability. Lateral channel adjustment can take many forms. A river can widen a channel by eroding channel banks and valley walls; it can migrate across the valley floor and mine channel-bed and floodplain sediment without causing significant incision; or it can entrain sediment delivered to the channel from external sources, such as from tributary channels or extrafluvial mass failures. All of these types of adjustments are evident at Mount St. Helens.

Since construction of the SRS, several DEMs of all or part of the debris-avalanche deposit have been created from aerial photography and lidar surveys to assess topographic change. Some of these DEMs have been used to produce DEMs of difference (DoDs) (Wheaton et al. 2010) in order to assess spatial distributions of erosion and deposition and to quantify volumetric topographic changes and compute morphological sediment budgets (Bradley et al. 2001). DoDs are produced by subtracting the elevations of pixels in one DEM from those of corresponding pixels in a later DEM. Such

differencing provides the net vertical change between matched pixels. A net negative vertical change (erosion) does not necessarily represent vertical incision. Lateral erosion between times of DEMs can also produce net negative vertical change. This is particularly evident where large magnitudes of net erosion along a channel or valley margin are juxtaposed with substantially lesser magnitudes of net erosion (or even deposition) on a valley floor. Here, we compare and contrast a DoD representing topographic changes during the second decade after the 1980 eruption (1987–1999 DoD) with one that represents changes during the third decade after eruption (1999–2009 DoD).

Bradley et al. (2001) produced a DoD from DEMs of the debris-avalanche surface derived from aerial photographs obtained in 1987 and 1999. However, neither they nor the more comprehensive report which their work summarizes (West Consultants 2002) provides vertical accuracies of the DEMs or uncertainty of the DoD. We therefore recreated a 1987–1999 DoD having quantified uncertainty and a stated change-detection limit. We also created a 1999–2009 DoD from the 1999 DEM and a DEM based on a 2009 lidar survey (Mosbrucker 2014).

2.5.1 Estimates of Error in the DEMs and Resulting DoDs

One of the most useful aspects of a DoD is its ability to quantify volumetric change. However, quantitative estimates of erosion and deposition are subject to errors within each DEM and to the propagation of those individual errors to the DoD. The metadata that accompanied the original 1987 and 1999 DEMs provide scales of photographs acquired, intended scales of topographic maps to be generated from the photography, target contour intervals, and photogrammetric points from which the topographic maps and DEMs were derived. Those metadata do not provide estimates of vertical accuracies. The 1987 and 1999 photographs were acquired to support 1:2400-scale contour maps having a 1.22-m (4-ft) contour interval. Photogrammetric point densities support DEM resolutions of about 20 m, but West Consultants (2002) generated DEMs using triangulated irregular networks (TINs) interpolated to 3-m-grid resolution.

Because the vertical accuracies of the 1987 and 1999 DEMs are not specified, they must be estimated. We can estimate approximate vertical accuracy of the DEMs if we assume that the underlying photography met appropriate specifications and that photogrammetric techniques were properly executed when the consequent points, maps, and DEMs were compiled. The National Map Accuracy Standard (NMAS) (Maune et al. 2001), as applied to contour maps, specifies that elevation differences of no more than 10% of tested, well-defined points on a map may exceed one-half the contour interval. Thus, the intended map scales of the photography and target contour intervals suggest vertical accuracies of at least 0.61 m at the 90% confidence level. The American Society for Photogrammetry and Remote Sensing (ASPRS) further refined vertical accuracy standards for contour maps. The ASPRS standard (ASPRS 1990; Maune et al. 2001) for a class 1 contour map (the most accurate) states that the limiting root-mean-square vertical error ($RMSE_z$) for well-defined features between contours is one-third the contour interval. If the photography and consequent map compilations met that standard, then the intended map scales and target contour intervals suggest a limiting $RMSE_z$ of 0.41 m. However, these standards apply to contour maps, and neither is directly applicable to DEMs. The National Standard for Spatial Data Accuracy (NSSDA) of 1998 is specifically designed to be applied to digital geospatial data (Maune et al. 2001). Vertical accuracy of a DEM at the 95% confidence interval according to NSSDA standards can be related to NMAS vertical accuracy and ASPRS limiting $RMSE_z$ standards for contour maps by (Maune et al. 2001):

$$\text{Accuracy}_z\left(\text{NSSDA}\right) = 1.1916 \times \text{NMAS vertical accuracy} \tag{2.1}$$

$$\text{Accuracy}_z\left(\text{NSSDA}\right) = 1.9600 \times \text{RMSE}_z \tag{2.2}$$

Equation (2.1) can be related to map contour interval by:

$$\text{Accuracy}_z\left(\text{NSSDA}\right) = 1.1916 \times \left(\begin{matrix}0.5 \times \text{contour} \\ \text{interval}\end{matrix}\right) \tag{2.3}$$

$$\text{Accuracy}_z\left(\text{NSSDA}\right) = 0.5958 \times \text{contour interval} \tag{2.4}$$

If we assume that vertical errors are normally distributed and that the photography and mapping that support the DEMs met their intended scales and contour intervals, then the estimated vertical accuracies of the 1987 and 1999 DEMs at the 95% confidence level range from 0.73 to 0.80 m (Eqs. 2.2 and 2.4). From 2010 to 2012, we spot-checked elevations in the DEMs along North Fork Toutle valley in the vicinity of Coldwater Lake in places that had not changed since the photographs were acquired. Those limited field checks confirm that our estimate of vertical accuracies of those DEMs is reasonable but probably a bit high.

The 2009 lidar-derived DEM has higher resolution and greater vertical accuracy than those derived from aerial photographs. The report accompanying the 2009 lidar survey states that the DEM has a 1-m resolution, and vertical accuracy obtained from spot checks along a bare road surface is 0.071 m at the 95% confidence level (Mosbrucker 2014). Spot checks of 103 elevations on the surface of the debris-avalanche deposit, however, show a lower accuracy on natural terrain; there, the DEM has a vertical accuracy ranging

from 0.10 to 0.50 m at the 95% confidence level, with a mean accuracy of 0.35 m (Mosbrucker 2014). To match the interpolated resolution of the 1987 and 1999 DEMs, we degraded the 2009 DEM to 3-m-grid resolution.

Estimates of volumetric change in sediment erosion and deposition are computed by subtracting surface elevations of one DEM from those of another. However, measurements of change between two DEMs incorporate errors of each DEM. Therefore, potential vertical error of the DoD must be estimated in order to determine the minimum level of change that distinguishes detectable change from noise.

Simple error propagation (Bevington 1969; Brasington et al. 2003) is used to determine the minimum level of change detection in the DoD. Errors from individual DEMs are propagated into the DoD as:

$$\delta_{\mathrm{DoD}} = \sqrt{\delta_{\mathrm{old}}^2 + \delta_{\mathrm{new}}^2} \tag{2.5}$$

where δ_{DOD} is the propagated vertical error in the DoD, δ_{old} is the vertical error of the earlier DEM, and δ_{new} is the vertical error of the later DEM. This estimate of propagated error assumes that errors are normally distributed and those for each cell of each DEM are random and independent.

We compute the estimated error of the recreated 1987–1999 DoD using an approximate value of the estimated vertical accuracy of each DEM. Substituting a midrange value (0.75 m) of the estimated vertical accuracy for the 1987 and 1999 DEMs into Eq. 2.5 yields an estimated δ_{DOD} of 1.06 m. Hence, propagation of estimated vertical accuracies of the individual DEMs indicates our 1987–1999 DoD has a threshold level of change detection of about 1 m. Using the midrange value of estimated vertical accuracy for the 1999 DEM and the range of vertical accuracy values at the 95% confidence level for the 2009 DEM indicates the threshold level of change detection in the 1999–2009 DoD ranges from 0.75 to 0.90 m, a level of detection that is influenced largely by the assumed vertical accuracy of the 1999 DEM. Because the propagated vertical accuracy in the 1999–2009 DoD is influenced so strongly by assumed accuracy of the 1999 DEM, and because vertical accuracy of the 1999 DEM is based on many assumptions, we also use 1 m as the threshold level of change detection for the 1999–2009 DoD. Therefore, in both the 1987–1999 and 1999–2009 DoDs we produced, vertical elevation changes of less than 1 m are considered noise. That change-detection threshold appears reasonable for changes on the valley floor and in areas of high point density. However, it may be too low in areas of low point density ($\leq$1 point per m^2) such as on valley slopes greater than 30° or under locally heavy vegetation. We thus restrict our analyses of change to the valley bottom. This restriction loses little information of relevance because steep valley slopes that bound the debris-avalanche deposit contribute little sediment to the river.

2.5.2 Topographic Changes from 1987 to 1999

Like Bradley et al. (2001), we find that there was net erosion from 1987 to 1999 along the entire North Fork Toutle River channel system upstream of the former N1 structure—a small sediment-retention structure built upstream of the SRS in the early 1980s (Willingham 2005; Fig. 2.7). Documented net erosion includes an 8-km-long reach downstream of Elk Rock (Fig. 2.7) where the valley widens considerably—a reach where Simon (1999) and Zheng et al. (2014) documented predominantly channel-bed aggradation (e.g., NF375; Fig. 2.4). By 1999, channel area had developed across 20% of the debris-avalanche deposit. However, the boundary of the DoD does not extend all the way to the lip of the crater because the 1987 photography did not extend that far. Thus, erosion along Loowit channel from the mid-Pumice Plain (approximately cross section LO030) to the crater lip (Figs. 2.2 and 2.7) is unaccounted in the analysis. The documented erosion in the DoD is thus a minimum volume within the valley.

Much of the erosion documented from 1987 to 1999 was focused locally (Table 2.1; Fig. 2.7). The greatest erosion occurred along North Fork Toutle River channel from near Elk Rock to about its confluence with Castle and Coldwater Creeks (Table 2.1 and Fig. 2.7). Other significant erosion occurred along Castle Creek and Coldwater Creek channels and locally along North Fork Toutle River channel upstream of the Castle Creek/Coldwater Creek confluence (Fig. 2.7 and Table 2.1). Channel erosion between Elk Rock and the Castle Creek/Coldwater Creek confluence accounted for about 40% of the volume eroded during the second decade after the 1980 eruption, even though this reach accounted for only about 20% of the active channel area (~4% of the area of the avalanche deposit). Castle Creek and Coldwater Creek channels combined accounted for nearly as much active channel area (17%) as did the reach from Elk Rock to the Castle/Coldwater confluence, but they contributed only about half as much sediment volume. By contrast, channel erosion above the Castle Creek/Coldwater Creek confluence—about 30% of the active channel area within the boundary of the DoD (~7% of the area of the avalanche deposit)—accounted for 28% of the volume eroded (Fig. 2.7 and Table 2.1). About 10% of documented erosion was downstream of Elk Rock (Table 2.1), and a very minor amount of erosion (about 1%) was from re-entrainment of sediment deposited behind the SRS.

Comparisons of net vertical changes detected by differencing the DEMs with measured changes in channel cross sections (e.g., Fig. 2.4) show that much of the channel change from 1987 to 1999 resulted from lateral bank erosion. The most extensive bank erosion occurred at the outsides of channel bends (Fig. 2.7). Locally, tens to hundreds of meters of lateral bank erosion caused as much as 57 m of negative (erosional)

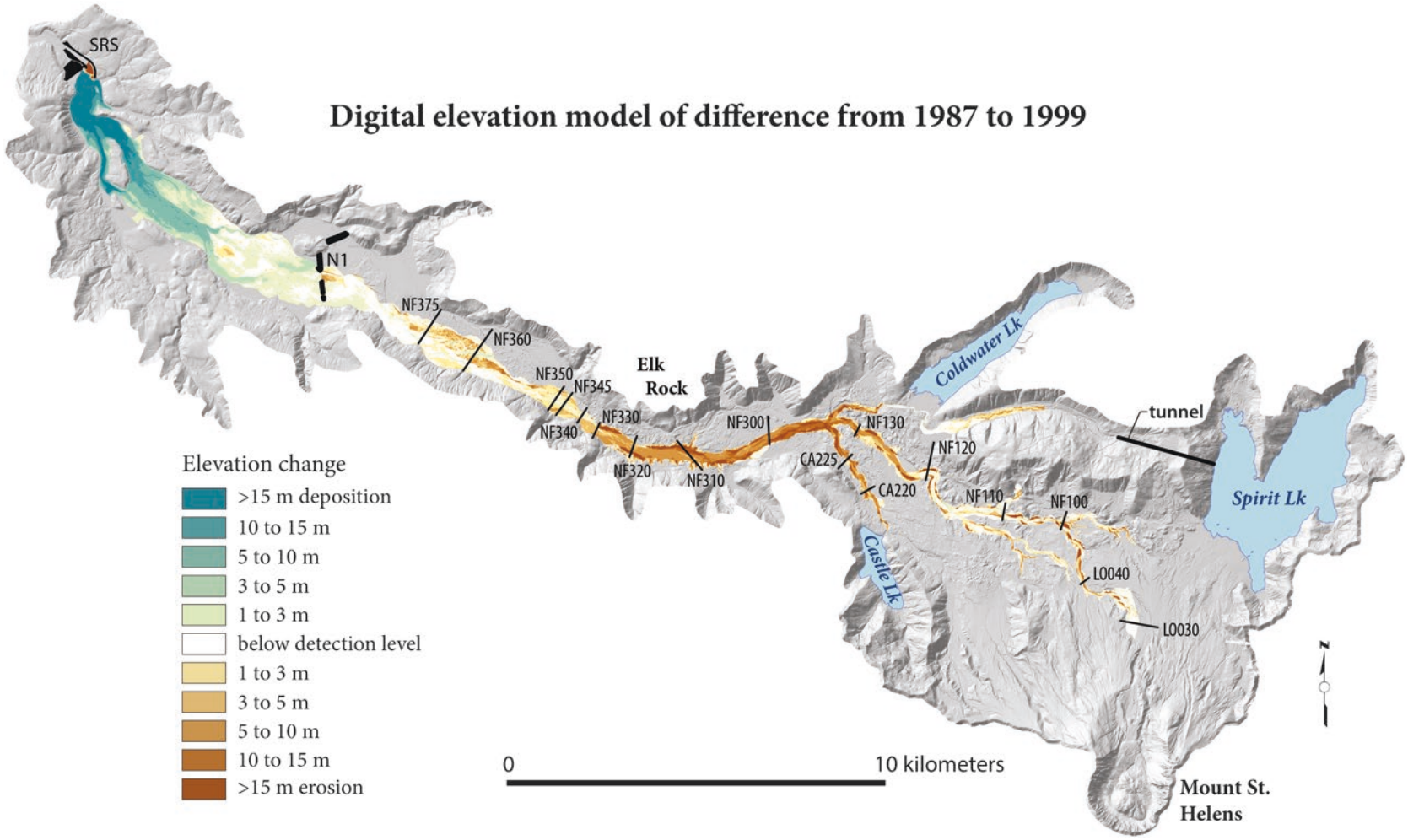

Fig. 2.7 Digital elevation model of topographic difference (DoD) created by differencing digital elevation models derived from aerial photography in 1987 and 1999 (see also Bradley et al. 2001). The DoD has been draped over a hill-shaded topographic model derived from a lidar survey in 2009. Locations of select cross sections shown (see Fig. 2.4). *SRS* is the location of sediment-retention structure completed in 1988. *N1* is the location of former small retention structure constructed in the early 1980s (see Willingham 2005). The deep erosion at SRS spillway is an artifact of construction activity; material had not yet been excavated at the time the 1987 photos were acquired.

Table 2.1 Comparison of results from DEMs of difference from 1987 to 1999 and 1999 to 2009.

	1987–1999				1999–2009			
Reach[a]	**Volume (million m^3)**[b]	**Area (million m^2)**[c]	**Average erosion yield**[d] **(m^3 m^{-2})**	**% of total erosion**	**Volume (million m^3)**	**Area (million m^2)**	**Average erosion yield (m^3 m^{-2})**	**% of total erosion**
Erosion								
Total above SRS	57.6 ± 1.3	23.8	2.4		38.9 ± 2.6	24.8	1.6	
Total erosion dilated by 16%[e]	66.8 ± 1.5				45.1 ± 3.0			
SRS–N1[f]	0.4 ± 0.2	9.8	0.04	1	0.9 ± 0.8	10.3	0.1	2
N1–NF340	6.9 ± 0.5	5.0 (3.5 on avalanche deposit)	1.4	12	6.2 ± 1.1	5.0 (3.5 on avalanche deposit)	1.2	16
NF340–NF/CA/CW confluence	22.4 ± 0.1	2.6	8.6	39	8.7 ± 0.1	2.0	4.4	22
NF/CA/CW–NF/TR/LO confluence[g]	12.4 ± 0.1	2.8	4.4	22	6.3 ± 0.2	2.8	2.3	16
Above NF/TR/LO confluence	3.6 ± 0.1	1.2	3.0	6	5.0 ± 0.04	1.2	4.2	13
Above LO030	–[h]	–	–	–	8.6 ± 0.04	1.7	5.1	22
Castle	7.4 ± 0.02	1.0	7.4	13	1.8 ± 0.1	0.6	3.0	5
Coldwater	4.5 ± 0.2	1.4	3.2	8	1.4 ± 0.3	1.2	1.2	4
Deposition								
SRS–N1	66.2 ± 0.6	9.8			14.7 ± 1.2	10.3		

[a]NF/CA/CW is the confluence of North Fork Toutle River, Castle Creek, and Coldwater Creek. NF/TR/LO is the confluence of North Fork Toutle River, Truman channel, and Loowit channel (see Fig. 2.2).
[b]Estimated from reanalysis of DEM of difference shown in Fig. 2.7. Values differ from those of Bradley et al. (2001) because we use a 1-m level-of-detection threshold.
[c]These values (and those for 1999–2009) represent areas of channel reworked or eroded by incision and migration. The area for SRS to N1 represents the total area of the sediment plain formed by deposition. Because channels there are braided, we did not compute specific areas of active channel erosion.
[d]Spatially averaged volume of sediment eroded per planimetric area of channel over the entire time period.
[e]To compare net erosion to values to net deposition, differences in deposit density must be taken into account. The average bulk density of the debris-avalanche deposit is 1.85 t m^{-3} (Glicken 1996). In general, bulk densities of fluvial deposits range from about 1.4 to 1.7 t m^{-3}. For computational purposes, Bradley et al. (2001) assumed a fluvial bulk density of 1.55 t m^{-3}—a value 16% less than the average density of the debris-avalanche deposit. Therefore, net erosion volumes are dilated 16% to compare with net deposition volumes.
[f]Although this reach is predominantly depositional, sediment was locally re-entrained.
[g]Computed volumes and channel areas include the Carbonate Springs reach (see Fig. 2.2).
[h]This reach is beyond the boundary of the 1987 DEM. Therefore, volumes of erosion cannot be computed.

vertical elevation change during this period as the river clawed into tall banks across the debris-avalanche deposit.

Even though channel widening was the dominant fluvial process during the second decade following eruption, thalweg elevation generally continued to change. Within and above the Elk Rock reach, thalweg elevation generally lowered but by locally variable amounts (Fig. 2.4; Zheng et al. 2014). By contrast to general channel degradation within and above the Elk Rock reach from 1987 to 1999, the sediment plain behind the SRS aggraded by as much as 36 m (Fig. 2.7). Despite the magnitudes of channel erosion, the overall longitudinal profile of North Fork Toutle River changed little between 1987 and 1999 except in the sediment plain behind the SRS (Bradley et al. 2001; Zheng et al. 2014). By this time, rates and magnitudes of channel incision had diminished considerably compared with the early 1980s, and most channel change was lateral. Locally persistent incision of a few meters or less had little effect on the overall channel profile (Simon 1999; Zheng et al. 2014; Mosbrucker et al. 2015). The documented dominance of lateral erosion, in conjunction with bed coarsening (Simon and Thorne 1996), rather than vertical incision during this period is consistent with Meyer and Martinson's (1989) conclusion that channel changes across much of the debris-avalanche deposit 5 years after the eruption were dominated mainly by channel widening accompanied by fluctuating, low-magnitude, vertical adjustments.

2.5.3 Morphological Sediment Budget Versus Measured Sediment Flux from 1987 to 1999

A morphological sediment budget obtained from estimates of net volume change in the DoD and measurements of sediment transport father downstream show the SRS trapped most sediment eroded from 1987 to 1999. The DoD shows 57.6 (±1.3) million m^3 of sediment eroded from upper North Fork Toutle valley and 66.2 (±0.6) million m^3 deposited in the sediment plain behind the SRS. This apparent discrepancy between erosion and deposition arises because the debris-avalanche sediment was deposited in a state denser than that typical of redeposited fluvial sediment. From several field measurements, Glicken (1996) found the mean bulk density of the debris-avalanche deposit is 1.85 t m^{-3}. By contrast, typical fluvial deposits have bulk densities that range from about 1.4 to 1.7 t m^{-3} (e.g., Wilcox et al. 2014; Warrick et al. 2015). Thus, sediment deposited behind the SRS likely has a bulk density that is probably 10–25% lower than that of the debris-avalanche deposit. To directly compare net erosion to net deposition, Bradley et al. (2001) used a 16% density difference (1.55 t m^{-3} or 88 lbs ft^{-3}, a mid-range density value commonly used for engineering purposes) to adjust net erosion volume, and we do likewise (Table 2.1). Thus, the density-adjusted net erosion was 66.8 (±1.5) million m^3. The morphological sediment budget therefore balances erosion and deposition. However, the DoD does not extend to the headwaters of the valley and therefore excludes erosion in the uppermost active channels. Also, erosion likely occurred below our change-detection limit. Furthermore, we know that a substantial amount of suspended sediment was transported downstream of the SRS from 1987 to 1999 (Major et al. 2000; Figs. 2.5 and 2.6). Therefore the volume of sediment eroded from the valley was greater than measured in the DoD.

Suspended-sediment discharge downstream of the SRS was measured on North Fork Toutle River (KID; Fig. 2.1) from 1982 to 1994, on South Fork Toutle River (SFT; Fig. 2.1) from 1982 to 2014, on Green River (GRE; Fig. 2.1) from 1982 to 1994, and along lower Toutle River (TOW) from 1981 to present (2015). From 1987 to 1994, 9.75 million t of suspended sediment passed KID, and 0.34 million t passed GRE, showing that North Fork Toutle River delivered 9.4 million t of suspended sediment below the SRS (Major et al. 2000). If we assume that after 1994 Green River delivered negligible sediment load, and that erosion between Green River confluence and TOW was negligible, then we can assume that the difference between suspended-sediment fluxes measured at TOW and SFT can be attributed to sediment delivery from North Fork Toutle River. The difference in fluxes between TOW and SFT from 1995 to 1999 is 9.2 million t (Major et al. 2000). Therefore, North Fork Toutle River delivered an estimated 18.6 million t of suspended sediment downstream of the SRS from 1987 to 1999. This estimate is probably accurate to within about 20% (Major 2004). If we assume bulk sediment density ranges from 1.4 to 1.7 t m^{-3}, then North Fork Toutle River delivered about 11–13 million m^3 of suspended sediment downstream of the SRS. Undetected erosion below our threshold limit and erosion upstream of the DoD boundary could easily balance this volumetric discrepancy. We therefore infer that about 80 million m^3 (density adjusted) of sediment eroded from upper North Fork Toutle River valley from 1987 to 1999 and that about 85% of that sediment accumulated behind the SRS.

2.5.4 Topographic Changes from 1999 to 2009

Cross sections of North Fork Toutle River along the debris-avalanche deposit (e.g., Figs. 2.2 and 2.8) show variable types and magnitudes of topographic change between 1999 and 2009. Although topographic changes in these sections are dominated by channel widening, channel incision continued to modify channel geometry. In general, magnitudes of incision were greatest and widening least upstream of the Elk Rock constriction, whereas magnitudes of widening were greatest and incision least downstream (generally above and below section NF345; Figs. 2.2 and 2.8). Channel incision outpaced lateral erosion at some sections along Loowit channel (LO040) and along the toe of the Pumice Plain (e.g., NF100 and NF110) (Figs. 2.2 and 2.8). Although channel incision is evident between sections NF120 and NF300 (Figs. 2.2 and 2.8), widening outpaced incision as that reach generally incised by only about 2 m but widened from a few tens to more than 100 m (e.g., NF300; Fig. 2.8). The greatest amounts of widening in this reach were between the Castle Creek/Coldwater Creek confluence and section NF300. Where the valley constricts near Elk Rock, the channel incised as much as 6 m but widened little (e.g., NF320; Fig. 2.8). Incision between NF300 and NF330 left abandoned terraces that narrowed the active channel. (Note the difference in active channel areas from 1987 to 1999 and from 1999 to 2009 above NF340 in Table 2.1. Also compare Figs. 2.7 and 2.9.) Where the valley widens downstream of the constriction, submeter- to meter-scale vertical fluctuations of the channel bed, caused by scour and fill, accompanied as much as 300 m of channel widening (e.g., NF345; Fig. 2.8). Here, the river transitions from a steep channel gradient past Elk Rock (about 20 m km^{-1}) to a much flatter gradient in the sediment plain behind the SRS (about 2.8 m km^{-1} from a few km downstream of former N1 retention structure to the SRS). Owing to this significant change in gradient, the river transitions from a single thread to a braided channel. As a result, hundreds of meters of lateral erosion of

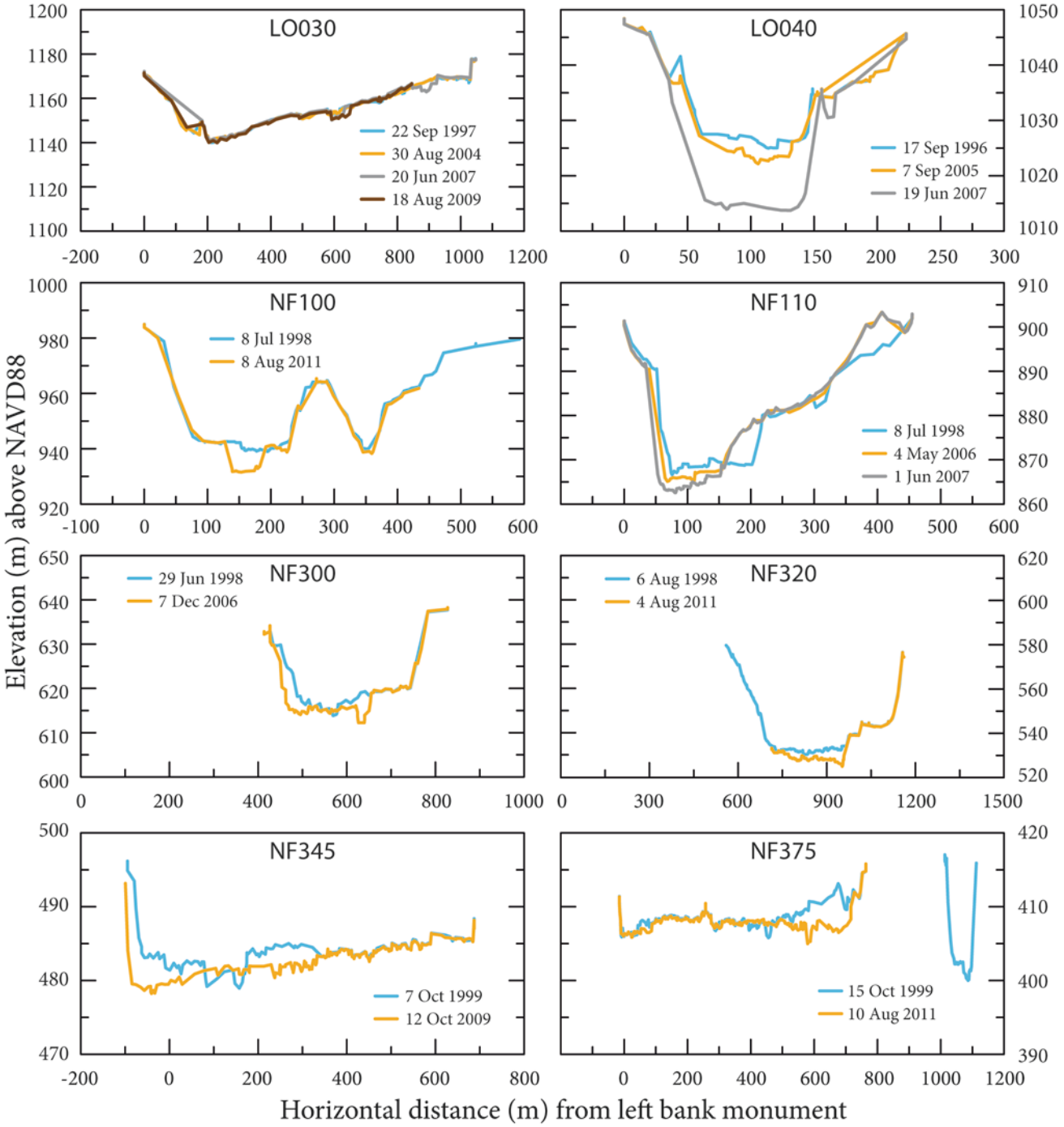

Fig. 2.8 Cross-section profiles from select locations on debris-avalanche deposit bounding the period 1999–2009. (See Figs. 2.2 and 2.9 for section locations. Also see Fig. 2.4 for channel geometry profiles prior to 1999).

relatively short (≤2–5-m-tall) banks and terraces (e.g., NF375; Fig. 2.8) dominated topographic changes.

Measurements of channel geometries along the debris-avalanche deposit show channel-bed elevation appears to have adjusted into a relatively stable profile by the third decade after the 1980 eruption (Zheng et al. 2014). Yet, sediment yield from North Fork Toutle catchment remains above probable pre-eruption level three decades after eruption (Fig. 2.6). The rapid reduction of sediment delivery from Green River catchment (Collins and Dunne 1986; Major et al. 2000; Major 2004) demonstrates that major catchments tributary to North Fork Toutle River are not the sources of persistently elevated

sediment yield. Thus, persistently high sediment delivery from North Fork Toutle River must result from in-channel processes or from reworking of sediment delivered to the channel by local mass failures. To obtain broader insights on topographic change in North Fork Toutle River valley above the SRS during the third decade after eruption, we compared the 1999 DEM to a 2009 lidar-derived DEM of the upper valley (Mosbrucker 2014).

The 1999–2009 DoD (Fig. 2.9) shows sediment erosion from the debris-avalanche deposit in the third decade after eruption was less voluminous and more spatially distributed than during the second decade (Figs. 2.7 and 2.9; Table 2.1). It also shows that the uppermost reaches of North Fork Toutle River headwater tributaries (Loowit Creek), reaches that were beyond the boundary of the 1987–1999 DoD, were erosional hotspots (Fig. 2.9). Most erosion between 1999 and 2009 (73%) was along North Fork Toutle River channel above Elk Rock and along Loowit channel (Figs. 2.2, 2.9 and Table 2.1). This reach of drainage accounted for about 50% of the active channel area across the avalanche deposit (~13% of the deposit area). The channels of Castle Creek and Coldwater Creek were much less active in the third decade after the eruption compared with the second decade. About 10% of erosion was along Castle Creek and Coldwater Creek (including South Coldwater Creek) channels combined, which account for 12% of active channel area. The remaining erosion was along North Fork Toutle River channel below Elk Rock. There, sediment was eroded not only from the channel above the former N1 retention structure (16%) but was also entrained from the sediment plain behind the SRS (2%; Table 2.1 and Fig. 2.9). After deposited sediment filled to the level of the SRS spillway in 1999, the sediment plain became a minor source for downstream sediment delivery.

Although erosion from 1999 to 2009 was more spatially distributed along the active channel system compared with erosion from 1987 to 1999, locally focused erosion was nevertheless important. Particular areas of focused erosion were along the volcano's lower north flank (upstream of cross section LO030), across the Pumice Plain (between cross sections LO030 and NF100), near Coldwater Lake between cross section NF120 and the Castle Creek/Coldwater Creek confluence, and near Elk Rock between cross sections NF310 and NF330 (Fig. 2.9). Downstream of NF120, erosion was focused particularly at channel bends. On the volcano's lower north flank, a few tens of meters of lateral bank erosion produced as much as 90 m of vertical elevation change because flow, strong winds, and mass failures gnawed away very tall banks, especially along upper Loowit Creek and Step Creek (Figs. 2.2 and 2.9). Oblique aerial photographs from late November 2006 indicate some, and perhaps much, of the documented erosion in upper Loowit Creek channel system happened during a large storm in early November 2006. Across the Pumice Plain, a few tens of meters of channel widening caused large changes in vertical elevation. Below the toe of the Pumice Plain (near cross section NF110; Fig. 2.9), a large mass failure of debris-avalanche sediment off Johnston Ridge in January 2006 deposited about 600 000 m^3 of sediment in the North Fork Toutle River channel. That deposit forced the river to erode laterally by tens of meters, which caused as much as 15–20 m of vertical elevation change. Near Elk Rock, channel shifting caused as much as 100–300 m of lateral bank erosion locally, and farther downstream it caused variable amounts of erosion. Magnitudes of valley-floor erosion diminished considerably downstream of cross section NF375 (Fig. 2.9).

Reaches of focused erosion along upper North Fork Toutle River channel were punctuated by reaches of substantive deposition (Fig. 2.9). At the base of the volcano's north flank, but above cross section LO030, as much as 4 m of deposit accumulated on the valley floor. Downstream of the fan of landslide debris that filled the channel near cross section NF110, fluvial and debris-flow deposits from the large storm in November 2006 left a 6-m-thick fill on the valley floor. Sediment transported during that storm also accumulated on the valley floor below cross section NF130 and displaced the confluence of North Fork Toutle River and Coldwater Creek several hundred meters downstream from its previous position. Below the former N1 retention structure, sediment deposition dominated changes in valley-floor topography although re-entrainment of previously deposited sediment is evident (Fig. 2.9). To minimize sediment re-entrainment and induce additional sedimentation behind the SRS, the US Army Corps of Engineers installed engineered log jams in 2010 (Townsend 2013) and raised the lip of the SRS spillway by 2.1 m in 2013.

Significantly less sediment eroded from upper North Fork Toutle River valley in the third decade after the 1980 eruption compared with the second. Total erosion measured upstream of the SRS between 1999 and 2009 (45 million m^3 density-adjusted) is about 60% of that eroded between 1987 and 1999 (67 million m^3 density-adjusted above the SRS plus about 12 million m^3 passed downstream) (Table 2.1). Furthermore, the proportion of eroded sediment that accumulated behind the SRS from 1999 to 2009 was substantially less than the proportion that accumulated from 1987 to 1999; only about 30% of eroded sediment volume accumulated behind the SRS from 1999 to 2009 (Table 2.1), whereas we infer about 85% accumulated from 1987 to 1999. That difference in relative proportion of sediment accumulation reflects the decrease in trap efficiency of the SRS, which by 1999 permitted most sediment delivered to the sediment plain to bypass the structure. Sediment that accumulated from 1999 to 2009 aggraded the sediment plain as much as 7 m, compared with 36 m of maximum aggradation from 1987 to 1999 when the SRS largely stored delivered sediment.

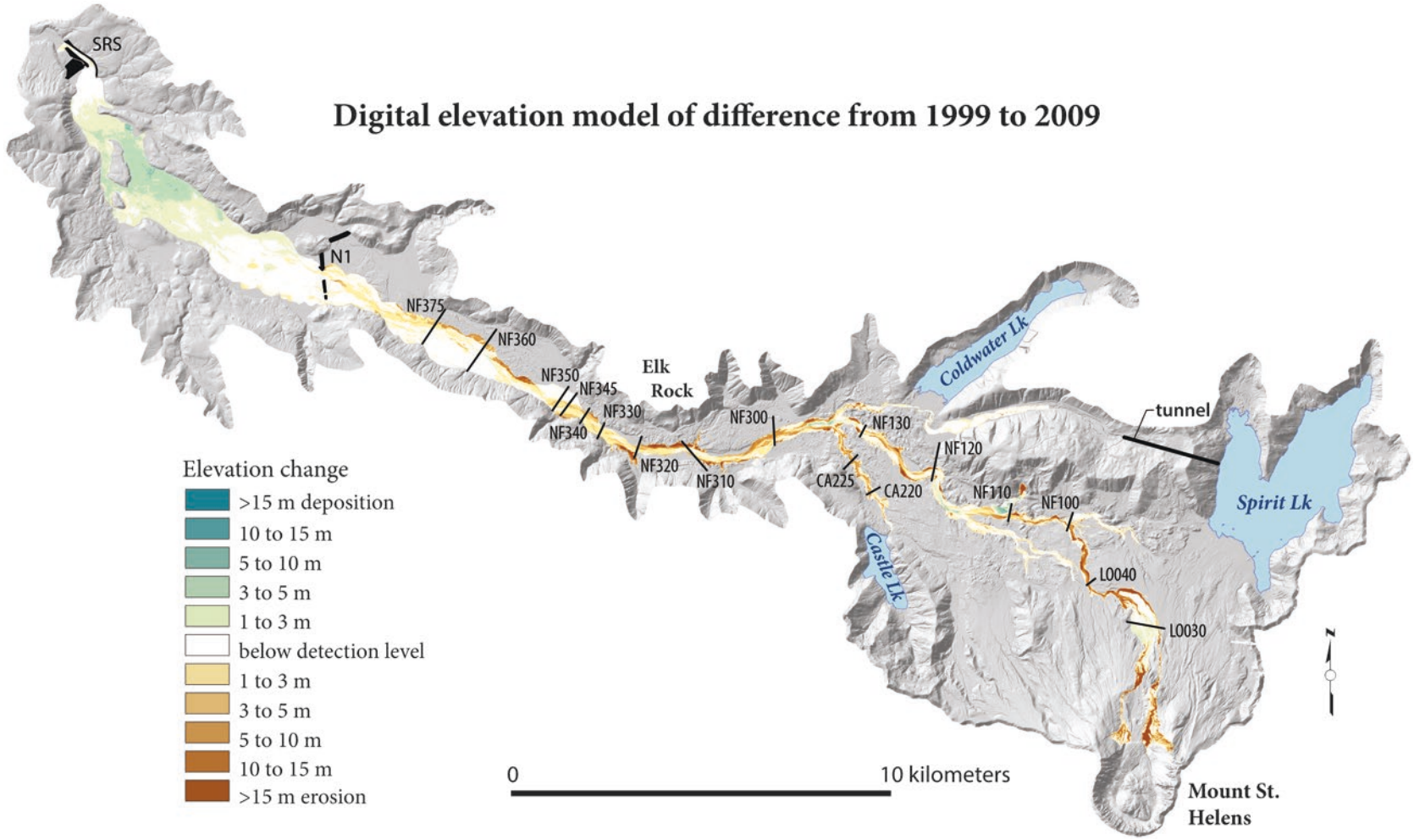

Fig. 2.9 Digital elevation model of topographic difference (DoD) created by differencing digital elevation models derived from aerial photography in 1999 (Bradley et al. 2001) and an airborne lidar survey in 2009 (Mosbrucker 2014). The DoD has been draped over a hill-shaded topographic model derived from the 2009 lidar survey. Locations of select cross sections shown (see Fig. 2.8). *SRS* is the location of sediment-retention structure completed in 1988. *N1* is the location of former small retention structure constructed in the early 1980s (see Willingham 2005).

2.5.5 Morphological Sediment Budget Versus Measured Sediment Flux from 1999 to 2009

The 1999–2009 DoD shows 38.9 (±2.6) million m^3 (45.1 ± 3.0 million m^3 density adjusted) net erosion from upper North Fork Toutle valley and 14.7 (±1.2) million m^3 net deposition behind the SRS (Table 2.1). Hence, the DoD shows about 30 (±1.8) million m^3 of sediment bypassed the SRS from 1999 to 2009, about three times the suspended-sediment load measured downstream and attributed to North Fork Toutle River from 1987 to 1999. By 1999, accumulated sediment had filled to the level of the SRS spillway, and substantial quantities of sediment, likely including sandy bedload, began passing the structure.

Fluxes of suspended sediment delivered by North Fork Toutle River downstream of the SRS after 1994 must be estimated by proxy because KID gauging station was decommissioned. Using the same assumptions as in Sect. 5.3, we estimate that North Fork Toutle River delivered about 15 million t of suspended sediment downstream of the SRS from 1999 to 2006. From 2007 to 2009, station FTP just downstream of the SRS (Fig. 2.1) measured 11.3 million t of suspended-sediment discharge (Fig. 2.5). Thus, from 1999 to 2009, North Fork Toutle River discharged about 26 million t, or 15–20 million m^3, of suspended sediment downstream of the SRS. That suspended-sediment load accounts for about 50–70% of the net sediment loss from upper North Fork Toutle River valley estimated from DoD analysis. The imbalance is most likely related to two main factors: (1) unmeasured bedload downstream of the SRS, and (2) fluvial storage of sediment between the SRS and TOW gauging station on lower Toutle River. Although the amount of bedload that may have passed the SRS is unknown, bedload typically comprises about 20% or more of total sediment load in steep mountain rivers, but proportions are highly variable (e.g., Wohl 2000; Major et al. 2012; Magirl et al. 2015). If we assume 20% of the load that passed the SRS was bedload, then net suspended-sediment loss from the upper valley is about 22–25 million m^3. If 20% of that potential suspended-sediment load was lost to channel, floodplain, and overbank storage between the SRS and TOW gauging station, then the amount of suspended-sediment load measured at TOW from 1999 to 2009 and attributed to North Fork Toutle River roughly balances net loss of suspended sediment estimated from the morphological sediment budget. Although these estimates of the fraction of sediment bypassing the SRS attributed to bedload and to suspended sediment lost to possible channel storage downstream are unconstrained, those processes provide a plausible explanation for the imbalance between the morphological sediment budget and suspended-sediment load measured downstream.

2.6 Discussion

Mount St. Helens' 1980 eruption severely disrupted the hydrogeomorphic conditions of Toutle River basin, in particular those of upper North Fork Toutle River valley. There, a massive debris-avalanche deposit reset valley topography. Its thick fill (average thickness of 45 m across 60 km^2), having a chaotic surface that lacked through-going flow, truncated confluences of tributary channels and hydrologically disconnected most of the upper valley (above the Green River confluence) from the channel downstream. An initial phase of rapid channel change across the debris-avalanche deposit ensued. Following channel initiation, incision and widening dominated channel change upstream of a valley constriction at Elk Rock (20 km down valley from the volcano), whereas aggradation and widening dominated downstream. During the early phase of channel evolution, North Fork Toutle River delivered sediment downstream at a rate several hundred times above pre-eruption levels. Concurrently, tephra erosion from hillsides in Green River catchment and lahar-deposit erosion along South Fork Toutle River channel augmented sediment delivery to lower Toutle River. Within 2 years of the eruption, each disturbed catchment achieved peak sediment delivery. Within 3–4 years, rates and magnitudes of hillside and channel erosion declined, and magnitudes of sediment delivery dropped sharply (Figs. 2.5 and 2.6). Magnitudes of sediment delivery were much less and rates of decline were more precipitous, from Green River catchment, where rills and gullies rapidly stabilized and hillside erosion swiftly diminished (Collins and Dunne 1986), and from South Fork Toutle catchment, where the river rapidly evacuated the most easily erodible lahar sediment (Meyer and Dodge 1988), than from North Fork Toutle catchment. Within 5 years of eruption, sediment delivery from Green River catchment returned to pre-eruption levels. Sediment delivery from South Fork Toutle catchment has fluctuated considerably over three decades since eruption (Fig. 2.6), caused largely by sensitive responses to storms that produced large floods. Although its level of sediment delivery may still be above pre-eruption levels, its average annual delivery since 2000 falls within the range of variation of sediment delivery from western Cascade Range rivers.

After 30 years, sediment delivery from upper North Fork Toutle River is far below its peak level of early 1980s but still many times above probable pre-eruption level. The great reduction of sediment delivery is due largely to diminished vertical incision, coarsening of the channel bed, and stabilization of the channel longitudinal profile, as well as to mitigation measures including construction of a massive sediment-retention structure (SRS). Analysis of thalweg elevations upstream of the SRS (Zheng et al. 2014) confirms

that changes in bed elevation were swift in the early 1980s but by 1987 had slowed considerably. From 1987 to 2009, the longitudinal profile of the channel changed little except where sediment accumulated behind the SRS. On the basis of observations and modeling, Zheng et al. (2014) inferred that relaxation of channel slope in conjunction with channel widening and bed coarsening reduced local stream power, which over time caused rates of vertical channel change to decrease and the profile of North Fork Toutle River to stabilize. Decades-long persistence of high sediment yield thus owes largely to ongoing channel widening, episodic extrafluvial input of mass failures, and reworking of the valley floor and floodplain through episodic avulsion and channel migration. Decades of repeated surveys of channel cross sections (e.g., Simon and Thorne 1996; Simon 1999; Mosbrucker et al. 2015) show that lateral erosion has been a dominant process sculpting the riverine landscape in upper North Fork Toutle River valley since the mid-1980s. Such prolonged channel instability, which maintains sediment transport at rates above pre-eruption levels but below peak rates immediately after eruptions, is a typical long-term fluvial geomorphic response to large explosive eruptions (Manville et al. 2009; Gran et al. 2011; Gran 2012; Pierson and Major 2014).

Patterns of topographic change across the debris-avalanche deposit were examined for two approximately decadal-scale periods—1987–1999 and 1999–2009—to assess spatial locations of ongoing channel instability and to quantify morphological sediment budgets. These periods are bracketed by digital elevation models that can be used to generate models of topographic difference (DoDs). Evident topographic changes show strong patterns of erosion and deposition. From 1987 to 1999, net channel erosion was highly focused along the channel of North Fork Toutle River in a reach 10–20 km downstream of the volcano as well as along Coldwater Creek and Castle Creek (Fig. 2.7). That reach of North Fork Toutle River coincides with some of the greatest changes in channel gradient relative to pre-eruption gradient (Simon 1999), and thus is an area where initial vertical changes of bed elevation were greatest. Rapid incision through that reach promoted bank instability, extensive lateral erosion, and channel braiding (Simon 1999). As the channel bed coarsened through the 1980s and early 1990s (Simon and Thorne 1996; Simon 1999) and rates of change of the channel longitudinal profile greatly diminished (Zheng et al. 2014), vertical incision through this steep-gradient reach became more difficult and lateral erosion more dominant. About 85% of the sediment eroded from 1987 to 1999 accumulated as thick fill immediately behind the SRS. By the third decade after the 1980 eruption (1999–2009), the channel profile along the debris-avalanche deposit had largely stabilized, hydraulic geometries of the channel system had largely adjusted to imposed sediment loads (Pitlick et al. 2006), and net channel changes caused by both vertical and lateral adjustments were of lesser magnitude and more spatially distributed (Fig. 2.9). Thus, by the third decade after eruption, the Elk Rock reach of North Fork Toutle River had become a less dominant sediment source. In contrast to the second decade after eruption, only about 30% of eroded sediment accumulated behind the SRS because fill had aggraded to the level of the structure's spillway. Between 1999 and 2009, trap efficiency of the SRS greatly diminished.

Net erosion of the fluvial system upstream of the SRS was about 40% less from 1999 to 2009 than from 1987 to 1999. This decline in net erosion resulted largely because channels eroded across the debris-avalanche deposit are wide (≥100 m wide) relative to flow footprints (bankfull flow about 10–20 m wide). As a result, the river and its headwater tributaries have less contact with steep channel banks and walls of valleys carved across the deposit than they did from 1987 to 1999 when channels were still actively evolving and adjusting width-to-depth ratios. Hydrological differences pose another possible cause of the large difference in net erosion between these periods. The period 1987–1999 contained a cycle of wetter-than-average conditions from 1995 to 1999 as well as floods of record in Toutle River basin in 1996 (Major 2004). In contrast, 1999–2009 was a cycle of generally drier-than-average conditions. But except for the 1996 flood, magnitudes and distributions of annual peak flows from 1987 to 1999 and from 1999 to 2009 were distributed similarly. Furthermore, average mean annual flow from 1999 to 2009 was only 5% less than that from 1987 to 1999 (57.2 $m^3\ s^{-1}$ versus 60.4 $m^3\ s^{-1}$ measured at TOW; see Fig. 2.6). These modest hydrological differences likely do not account for the large difference in net erosion between these two periods.

The rapid peak and sharp decline of sediment delivery from Toutle River basin followed by a decades-long phase of lower-level but still elevated sediment delivery (Figs. 2.5 and 2.6) is consistent with a posited conceptual model of geomorphic response following large explosive eruptions (Gran et al. 2011). In that model, the prolonged phase of geomorphic adjustments that causes persistently elevated sediment delivery is attributed to ongoing fluvial instability dominated by valley widening and reworking of the valley floor. Gran (2012) noted that seasonal influx and accumulation of sand on channel beds at Mount Pinatubo led to enhanced bed-sediment mobility and persistent low-level channel incision. From measured cross sections and observations at Mount St. Helens, Janda et al. (1984) and Simon (1999) noted that bank-toe erosion and mass wasting of bank materials caused large increases in channel width during early phases of channel evolution. Decadal-scale snapshots of spatial topographic changes at Mount St. Helens during the second and third decades after the 1980 eruption show the phase

of persistent fluvial instability along channels on the debris-avalanche deposit is dominated by bank failures leading to channel widening. Those snapshots show large vertical changes in elevation (many meters to tens of meters) accompanied only modest vertical degradation and even aggradation of adjacent channel floor—changes also documented by cross-section surveys. Such large net vertical changes in channel topography in a fluvial system experiencing diminishing rates of vertical bed-elevation change (Zheng et al. 2014) can be caused only by mass wasting of tall vertical banks and valley walls on the avalanche deposit.

Elevated sediment flux and lateral channel erosion provide a positive feedback loop that prolongs channel instability. Elevated sediment flux causes local channel-bed aggradation or sediment accumulation on channel bars, which distorts the flow field and establishes cross-stream gradients that drive flow toward opposing channel banks (Dunne et al. 2010; Wickert et al. 2013). Such flow-field distortion, along with conditions that promote mass failure of channel banks (e.g., toe erosion and elevated water tables), causes lateral bank erosion, which in turn introduces additional sediment to the river and increases sediment flux. As a result, the river channel remains dynamic and can maintain lateral migration (Dunne et al. 2010). Eventually, the developed floodplain becomes sufficiently wide and the active channel sufficiently narrow that the river only rarely flows against valley walls. By then, vegetation can stabilize channel banks, and the river mainly reworks its bed and floodplain within a zone of fairly consistent channel width. Gradually, channel mobility and sediment flux decrease until the system achieves a state of dynamic equilibrium (Wickert et al. 2013). In the case of volcanically disturbed river systems, and as is evident at Mount St. Helens, this state of equilibrium can take decades, perhaps centuries, to achieve (Gran et al. 2011; Pierson et al. 2011; Meadows 2014; Pierson and Major 2014).

Although the debris-avalanche deposit provides an enormous source of erodible sediment to North Fork Toutle River and its headwater tributaries, most of that sediment is sequestered from erosion. As of 2010, only about 20% of the planimetric area of the avalanche deposit had been modified by riverine and local mass-failure processes (Table 2.1), and only about 13% of the deposit volume had been eroded. Most likely, sediment outside the narrowly focused corridor that North Fork Toutle River and its headwater tributaries occupy will remain in place as channel mobility diminishes, floodplains develop, and forest and riparian vegetation recolonize the deposit and floodplain surfaces. Comparison of the 1987–1999 and 1999–2009 DoDs shows the overall position and shape of the river corridor has changed little in the second and third decades following the 1980 eruption.

2.7 Conclusions

More than 30 years after the 1980 eruption of Mount St. Helens, high sediment load continues to be released from Toutle River basin. Nearly all elevated load comes from persistent channel erosion across the debris-avalanche deposit that fills upper North Fork Toutle River valley. Sediment discharge by Green River, from a catchment having hillsides deforested and thinly draped with volcanic sediment by the blast PDC, returned to pre-eruption levels within 5 years after the eruption. Sediment discharge by South Fork Toutle River, reamed by a large (14 million m^3) lahar, has fluctuated greatly over three decades since the eruption. Although its sediment discharge may still be above pre-eruption levels, its average annual discharge has been within the range of variation of western Cascade Range rivers since 2000. Measurements of suspended-sediment discharge along North Fork Toutle River below a massive sediment-retention structure (SRS) and along lower Toutle River show that average sediment yield from North Fork Toutle River catchment remains more than ten times greater than probable pre-eruption level even with the presence of upstream mitigation measures.

Since the mid-1980s, channel change across the debris-avalanche deposit has been dominated by lateral channel adjustments. Although channel-bed incision has persisted within and upstream of a valley constriction near Elk Rock (20 km downstream of the volcano), the rate of bed-elevation change has diminished, and magnitudes of lateral erosion have generally outpaced those of incision.

Comparisons of digital elevation models from 1987, 1999, and 2009 reveal patterns of topographic changes across the debris-avalanche deposit in the second and third decades after the 1980 eruption. A digital elevation model of topographic difference (DoD) shows that channel erosion during the second decade after eruption (1987–1999) was strongly focused along a 6-km-long channel reach at and upstream of the valley constriction near Elk Rock and in the channels of Castle Creek and Coldwater Creek. During the third decade after eruption (1999–2009), a DoD shows erosion was more spatially distributed throughout the channel system. In conjunction with channel cross sections that show diminishing channel incision above Elk Rock and channel-bed aggradation below, those DoDs show large fractions of topographic changes resulted from lateral erosion owing to mass failure of tall banks.

Net erosion from the debris-avalanche deposit from 1999 to 2009 was about 40% less than that from 1987 to 1999. However, unlike the second decade after the eruption, when only about 15% of eroded sediment passed the SRS, nearly 70% of eroded sediment passed the SRS from 1999 to 2009, because by 1999, sediment fill behind the SRS had reached its spillway. Comparison of a morphological sediment budget developed

from the 1999–2009 DoD with measured suspended-sediment discharge downstream of the SRS indicates that sediment bypassing the SRS (largely sand) may have moved downstream as unmeasured bedload and some suspended sediment may have been stored along the channel or on the floodplain between the SRS and lower Toutle River valley.

The active river corridor has sculpted only about 20% of the surface of the debris-avalanche deposit. Because of the vertical depth of that corridor, large areas of the avalanche deposit will remain sequestered from fluvial processes. Diminishing topographic changes in areas affected by fluvial processes indicate that parts of the drainage network across the deposit are stabilizing.

Acknowledgments We thank the US Army Corps of Engineers Portland District Office for generously providing us digital elevation data for 1987, 1999, and 2009. Dennis Saunders and Tami Christianson helped us compile suspended-sediment and cross-section data. Tim Meadows, Jim O'Connor, Charles Crisafulli, and two anonymous reviewers provided comments that improved this chapter.

Glossary

Blast pyroclastic density current A form of pyroclastic density current initiated by rapid decompression of lava domes or cryptodomes (magma bodies cooled high within a volcanic edifice) owing to sudden collapse. Rapid decompression results in a directed explosion that initially impels the current laterally before it becomes a gravity-driven flow [Sources: a generalized definition based on definitions of PDCs provided in Pierson and Major 2014, Sigurdsson et al. (2015)]. In the case of the Mount St. Helens 1980 eruption, failure of the volcano's north flank unroofed pressurized magma and superheated water. Rapid exsolution of magmatic gases and conversion of superheated water to steam produced a laterally directed blast, which formed a density current that flowed across rugged topography. The current contained fragmented rock debris as well as shattered forest material (Lipman and Mullineaux 1981).

Debris avalanche A rapid granular flow of an unsaturated or partly saturated mixture of volcanic rock particles (± ice) and water, initiated by the gravitational collapse and disintegration of part of a volcanic edifice. Debris avalanches differ from debris flows in that they are not water saturated. Although debris avalanches commonly occur in association with eruptions, they can also occur during periods when a volcano is dormant. Sources: Pierson and Major (2014), Sigurdsson et al. (2015).

Lahar An Indonesian term for a rapid granular flow of a fully saturated mixture of volcanic rock particles (± ice), water, and commonly woody debris. A lahar that has ≥50% solids by volume is termed a *debris flow*; one that has roughly 10–50% solids by volume is termed a *hyperconcentrated flow*. Flow type can evolve with time and distance along a flow path as sediment is entrained or deposited. Sources: Pierson and Major (2014), Sigurdsson et al. (2015).

Pyroclastic density current (PDC) Rapid flow of a dry mixture of hot (commonly >700 °C) solid particles, gases, and air, which can range in character from a dense, ground-hugging flow (*pyroclastic flow*) to a turbulent, low-density cloud of mostly fine ash and superheated air (*pyroclastic surge*). A single PDC commonly involves both flow types as a result of gravitational segregation. Flows are generally gravity driven but may be accelerated initially by impulsive lateral forces of directed volcanic explosions. Flows typically move at high velocity (up to several hundred km h^{-1}). Source: Pierson and Major (2014).

Pyroclastic flow See pyroclastic density current (PDC).

Tephrafall A rain of volcanic particles to the ground following ejection into the atmosphere by an explosive eruption. Tephra is a collective term for particles of any size, shape, or composition ejected in an explosive eruption. Sources: Pierson and Major (2014), Sigurdsson et al. (2015).

References

ASPRS. 1990. ASPRS accuracy standards for large-scale maps. *Photogrammetric Engineering and Remote Sensing* 56: 1068–1070.

Beget, J.E. 1982. *Postglacial volcanic deposits at Glacier Peak, Washington, and potential hazards from future eruptions*, Open-File Report 82–830. Washington, DC: U.S. Geological Survey.

Belousov, A., B. Voight, and M. Belousova. 2007. Directed blasts and blast-generated pyroclastic density currents: A comparison of the Bezymianny 1956, Mount St. Helens 1980, and Soufrière Hills, Montserrat 1997 eruptions and deposits. *Bulletin of Volcanology* 69: 701–740.

Bevington, P.R. 1969. *Data reduction and error analysis for the physical sciences*. New York: McGraw-Hill.

Bradley, J.B., T.R. Grindeland, and H.R. Hadley. 2001. *Sediment supply from Mount St. Helens—20 years later*. Proceedings of the Seventh Federal Interagency Sedimentation Conference, March 25–29, 2001, Reno, Nevada, USA, volume 2: x-9–x-16.

Brand, B.D., C. Mackaman-Lofland, N.M. Pollock, S. Bendaña, B. Dawson, and P. Wichgers. 2014. Dynamics of pyroclastic density currents: Conditions that promote substrate erosion and self-channelization—Mount St. Helens, Washington (USA). *Journal of Volcanology and Geothermal Research* 276: 189–214.

Brasington, J., J. Langham, and B. Rumsby. 2003. Methodological sensitivity of morphometric estimates of coarse fluvial sediment transport. *Geomorphology* 53: 299–316.

Christiansen, R.L., and D.W. Peterson. 1981. The 1980 eruptions of Mount St. Helens. In *The 1980 eruptions of Mount St. Helens, Washington*, Professional Paper 1250, ed. P.W. Lipman and D.R. Mullineaux, 15–51. Washington, DC: U.S. Geological Survey.

Collins, B.D., and T. Dunne. 1986. Erosion of tephra from the 1980 eruption of Mount St. Helens. *Geological Society of America Bulletin* 97: 896–905.

Crandell, D.R. 1987. *Deposits of pre-1980 pyroclastic flows and lahars from Mount St. Helens volcano, Washington*, Professional Paper 1444. Washington, DC: U.S. Geological Survey.

Criswell, C.W. 1987. Chronology and pyroclastic stratigraphy of the May 18, 1980 eruption of Mount St. Helens, Washington. *Journal of Geophysical Research* 92: 10,237–10,266.

Czuba, J.A., C.S. Magirl, C.R. Czuba, E.E. Grossman, C.A. Curran, A.S. Gendaszek, and R.S. Dinacola. 2011. *Sediment load from major rivers into Puget Sound and its adjacent waters*, Fact Sheet 2011-3083. Washington, DC: U.S. Geological Survey.

Dale, V.H., F.J. Swanson, and C.M. Crisafulli. 2005a. Disturbance, survival, and succession: Understanding ecological responses to the 1980 eruption of Mount St. Helens. In *Ecological responses to the 1980 eruption of Mount St. Helens*, ed. V.H. Dale, F.J. Swanson, and C.M. Crisafulli, 3–11. New York: Springer.

———, eds. 2005b. *Ecological responses to the 1980 eruption of Mount St. Helens*. New York: Springer.

Dinehart, R.L. 1998. *Sediment transport at gaging stations near Mount St. Helens, Washington, 1980–1990: Data collection and analysis*, Professional Paper 1573. Washington, DC: U.S. Geological Survey.

Dunne, T., J.A. Constantine, and M.B. Singer. 2010. The role of sediment transport and sediment supply in the evolution of river channel and floodplain complexity. *Transactions of the Japanese Geomorphological Union* 31 (2): 155–170.

Esposti Ongaro, T., A.B. Clarke, B. Voight, A. Neri, and C. Widiwijayanti. 2012. Multiphase flow dynamics of pyroclastic density currents during the May 18, 1980 lateral blast of Mount St. Helens. *Journal of Geophysical Research* 117: B06208. https://doi.org/10.1029/2011JB009081.

Fairchild, L.H. 1987. The importance of lahar initiation processes. In *Debris flows/avalanches: Process, recognition, and mitigation*, Reviews in Engineering Geology, ed. J.E. Costa and G.F. Wieczorek, vol. VII, 51–61. Boulder: Geological Society of America.

Gabet, E.J., O.J. Reichman, and E.W. Seabloom. 2003. The effects of bioturbation on soil processes and sediment transport. *Annual Review of Earth and Planetary Sciences* 31: 249–273.

Glicken, H.X. 1996. *Rockslide-debris avalanche of May 18, 1980, Mount St. Helens Volcano, Washington*, Open-File Report 96–677. Washington, DC: U.S. Geological Survey.

Gran, K.B. 2012. Strong seasonality in sand loading and resulting feedbacks on sediment transport, bed texture, and channel planform at Mount Pinatubo, Philippines. *Earth Surface Processes and Landforms* 37: 1012–1022.

Gran, K.B., and D.R. Montgomery. 2005. Spatial and temporal patterns in fluvial recovery following volcanic eruptions—Channel response to basin-wide sediment loading at Mount Pinatubo, Philippines. *Geological Society of America Bulletin* 117: 195–211.

Gran, K.B., D.R. Montgomery, and J.C. Halbur. 2011. Long-term elevated post-eruption sedimentation at Mount Pinatubo. *Geology* 39: 367–370.

Hardison, J.H. III. 2000. *Post-lahar channel adjustment, Muddy River, Mount St. Helens, Washington*. M.S. thesis. Fort Collins: Colorado State University.

Hoblitt, R.P., C.D. Miller, and J.W. Vallance. 1981. Origin and stratigraphy of the deposit produced by the May 18 directed blast. In *The 1980 eruptions of Mount St. Helens, Washington*, Professional Paper 1250, ed. P.W. Lipman and D.R. Mullineaux, 401–420. Washington, DC: U.S. Geological Survey.

Janda, R.J., K.M. Scott, K.M. Nolan, and H.A. Martinson. 1981. Lahar movement, effects, and deposits. In *The 1980 eruptions of Mount St. Helens, Washington*, Professional Paper 1250, ed. P.W. Lipman and D.R. Mullineaux, 461–478. Washington, DC: U.S. Geological Survey.

Janda, R.J., D.F. Meyer, and D. Childers. 1984. Sedimentation and geomorphic changes during and following the 1980–1983 eruptions of Mount St. Helens, Washington. *Shin Sabo* 37 (2): 10–21 and 37(3): 5–19.

Johnson, M.G., and R.L. Beschta. 1980. Logging, infiltration capacity, and surface erodibility in western Oregon. *Journal of Forestry* 78: 334–337.

Jones, J.A. 2000. Hydrologic processes and peak discharge response to forest removal, regrowth, and roads in 10 small experimental basins, western Cascades, Oregon. *Water Resources Research* 36: 2621–2642.

Leavesley, G.H., G.C. Lusby, and R.W. Lichty. 1989. Infiltration and erosion characteristics of selected tephra deposits from the 1980 eruption of Mount St. Helens, Washington, USA. *Hydrological Sciences Journal* 34: 339–353.

Lipman, P.W., and D.R. Mullineaux, eds. 1981. *The 1980 eruptions of Mount St. Helens, Washington*, Professional Paper 1250. Washington, DC: U.S. Geological Survey.

Lisle, T.E. 1995. Effects of coarse woody debris and its removal on a channel affected by the 1980 eruption of Mount St. Helens, Washington. *Water Resources Research* 31: 1797–1808.

Lombard, R.E., M.B. Miles, L.M. Nelson, D.L. Kresch, and P.J. Carpenter. 1981. The impact of mudflows of May 18 on the lower Toutle and Cowlitz Rivers. In *The 1980 eruptions of Mount St. Helens, Washington*, Professional Paper 1250, ed. P.W. Lipman and D.R. Mullineaux, 693–699. Washington, DC: U.S. Geological Survey.

Magirl, C.S., R.C. Hilldale, C.A. Curran, J.J. Duda, T.D. Straub, M. Domanski, and J.R. Foreman. 2015. Large-scale dam removal on the Elwha River, Washington, USA: Fluvial sediment load. *Geomorphology* 246: 669–686.

Major, J.J. 2004. Posteruption suspended sediment transport at Mount St. Helens: Decadal-scale relationships with landscape adjustments and river discharges. *Journal of Geophysical Research* 109: F01002. https://doi.org/10.1029/2002JF000010.

Major, J.J., and L.E. Lara. 2013. Overview of Chaitén Volcano, Chile, and its 2008–2009 eruption. *Andean Geology* 40: 196–215.

Major, J.J., and L.E. Mark. 2006. Peak flow responses to landscape disturbances caused by the cataclysmic 1980 eruption of Mount St. Helens, Washington. *Geological Society of America Bulletin* 118: 938–958.

Major, J.J., and K.M. Scott. 1988. *Volcaniclastic sedimentation in the Lewis River valley, Mount St. Helens, Washington—processes, extent, and hazards*, Bulletin 1383-D. Washington, DC: U.S. Geological Survey.

Major, J.J., and T. Yamakoshi. 2005. Decadal-scale change of infiltration characteristics of a tephra-mantled hillslope at Mount St. Helens, Washington. *Hydrological Processes* 19: 3621–3630.

Major, J.J., T.C. Pierson, R.L. Dinehart, and J.E. Costa. 2000. Sediment yield following severe volcanic disturbance—a two-decade perspective from Mount St. Helens. *Geology* 28: 819–822.

Major, J.J., J.E. O'Connor, C.J. Podolak, M.K. Keith, G.E. Grant, K.R. Spicer, S. Pittman, H.M. Bragg, J.R. Wallick, D.Q. Tanner, A. Rhode, and P.R. Wilcock. 2012. *Geomorphic response of the Sandy River, Oregon, to removal of Marmot Dam*, Professional Paper 1792. Washington, DC: U.S. Geological Survey.

Manville, V. 2002. Sedimentary and geomorphic responses to ignimbrite emplacement: Readjustment of the Waikato River after the AD 181 Taupo eruption, New Zealand. *Journal of Geology* 110: 519–541.

Manville, V., K.A. Hodgson, and I.A. Nairn. 2007. A review of breakout floods from volcanogenic lakes in New Zealand. *New Zealand Journal of Geology and Geophysics* 50: 131–150.

Manville, V., B. Segschneider, E. Newton, J.D.L. White, B.F. Houghton, and C.J. Wilson. 2009. Environmental impact of the 1.8 ka Taupo eruption, New Zealand—Landscape responses to a large-scale explosive rhyolite eruption. *Sedimentary Geology* 220: 318–336.

Martinson, H.A., S.D. Finneran, and L.J. Topinka. 1984. *Changes in channel geomorphology of six eruption-affected tributaries of the Lewis River, 1980–82, Mount St. Helens, Washington*, Open-File Report 84-614. Washington, DC: U.S. Geological Survey.

Martinson, H.A., H.E. Hammond, W.W. Mast, and P.D. Mango. 1986. *Channel geometry and hydrologic data for six eruption-affected tributaries of the Lewis River, Mount St. Helens, Washington, water years 1983–84*, Open-File Report 85-631. Washington, DC: U.S. Geological Survey.

Maune, D.F., J. Binder Maitra, and E.J. McKay. 2001. Accuracy standards. In *Digital elevation model technologies and applications: The DEM users manual*, ed. D.F. Maune, 61–82. Bethesda: American Society for Photogrammetry and Remote Sensing.

McDonnell, J.J. 2003. Where does water go when it rains? Moving beyond the variable source area concept of rainfall-runoff response. *Hydrological Processes* 17: 1869–1875.

McGuire, K.J., J.J. McDonnell, M. Weiler, C. Kendall, B.L. McGlynn, J.M. Welker, and J. Siebert. 2005. The role of topography on catchment-scale water residence time. *Water Resources Research* 41: W05002. https://doi.org/10.1029/2004WR003657.

Meadows, T. 2014. Forecasting long-term sediment yield from the upper North Fork Toutle River, Mount St. Helens, USA. PhD. Thesis. Nottingham: University of Nottingham.

Meyer, D.F. 1995. *Stream-channel changes in response to volcanic detritus under natural and augmented discharge, South Coldwater Creek, Washington*, Open-File Report 94-519. Washington, DC: U.S. Geological Survey.

Meyer, D.F., and J.E. Dodge. 1988. *Post-eruption changes in channel geometry of streams in the Toutle River drainage basin, 1983–85, Mount St. Helens, Washington*, Open-File Report 87-549. Washington, DC: U.S. Geological Survey.

Meyer, D.F., and H.A. Martinson. 1989. Rates and processes of channel development and recovery following the 1980 eruption of Mount St. Helens, Washington. *Hydrological Sciences Journal* 34: 115–127.

Meyer, D.F., K.M. Nolan, and J.E. Dodge. 1986. *Post-eruption changes in channel geometry of streams in the Toutle River drainage basin, 1980–82, Mount St. Helens, Washington*, Open-File Report 85-412. Washington, DC: U.S. Geological Survey.

Miller, J.F., R.H. Frederick, and R.J. Tracey. 1973. *NOAA atlas 2, precipitation—frequency atlas of the western United States, Volume IX–Washington*. Silver Springs: U.S. Department of Commerce, National Oceanic and Atmospheric Administration, National Weather Service.

Moore, J.G., and T.W. Sisson. 1981. Deposits and effects of the May 18 pyroclastic surge. In *The 1980 eruptions of Mount St. Helens, Washington*, Professional Paper 1250, ed. P.W. Lipman and D.R. Mullineaux, 421–438. Washington, DC: U.S. Geological Survey.

Mosbrucker, A.R. 2014. *High-resolution digital elevation model of Mount St. Helens crater and upper North Fork Toutle basin, Washington, based on an airborne lidar survey of September 2009*, Data Series 904. Washington, DC: U.S. Geological Survey. https://doi.org/10.3133/ds904 .

Mosbrucker, A.R., K.R. Spicer, J.J. Major, D.R. Saunders, T.S. Christianson, and C.G. Kingsbury. 2015. *Digital database of channel cross-section surveys, Mount St. Helens, Washington*, Data Series 951. Washington, DC: U.S. Geological Survey. https://doi.org/10.3133/ds951.

Newhall, C.G., and R.S. Punongbayan, eds. 1996. *Fire and mud—eruptions and Lahars of Mount Pinatubo, Philippines*. Seattle: University of Washington Press.

O'Connor, J.E., P.F. McDowell, P. Lind, C.G. Rasmussen, and M.K. Keith. 2013. *Geomorphology and flood-plain vegetation of the Sprague and lower Sycan Rivers, Klamath basin, Oregon*, Scientific Investigations Report 2014-5223. Washington, DC: U.S. Geological Survey. http://doi.org/10.3133/sir20145223.

Paine, A.D.M., D.F. Meyer, and S.A. Schumm. 1987. Incised channel and terrace formation near Mount St. Helens, Washington. In *Erosion and Sedimentation in the Pacific Rim*, Publication 165, ed. R.L. Beschta, T. Blinn, G.E. Grant, F.J. Swanson, and G.G. Ice, 389–390. Christchurch: International Association of Hydrological Sciences.

Pierson, T.C., and J.J. Major. 2014. Hydrogeomorphic effects of explosive volcanic eruptions on drainage basins. *Annual Review of Earth and Planetary Sciences* 42: 469–507.

Pierson, T.C., P.T. Pringle, and K.A. Cameron. 2011. Magnitude and timing of downstream channel aggradation and degradation in response to a dome-building eruption at Mount Hood, Oregon. *Geological Society of America Bulletin* 123: 3–20.

Pitlick, J., J.J. Major, and K. Spicer. 2006. Morphodynamics of the North Fork Toutle River near Mount St. Helens. *EOS, Transactions of the Emerican Geophysical Union*, 87: Abstract H51G-0564.

Pringle, P.T., and K.A. Cameron. 1999. Eruption-triggered lahar on May 14, 1984. In *Hydrological consequences of hot-rock/snowpack interactions at Mount St. Helens Volcano, Washington 1982–84*, Professional Paper 1586, ed. T.C. Pierson, 81–103. Washington, DC: U.S. Geological Survey.

Pringle, P., and K. Scott. 2001. Postglacial influence of volcanism on the landscape and environmental history of the Puget Lowland, Washington—A review of geologic literature and recent discoveries, with emphasis on the landscape disturbances associated with lahars, lahar runouts, and associated flooding. In *Proceedings of the 2001 Puget Sound research conference*. ed. T. Droscher. Olympia: Puget Sound Water Quality Action Team. http://archives.eopugetsound.org/conf/2001PS_ResearchConference/sessions/oral/4d_pring.pdf. Last accessed 10 Feb 2014.

Roering, J.J., J. Marshall, A.M. Booth, M. Mort, and Q. Jin. 2010. Evidence for biotic controls on topography and soil production. *Earth and Planetary Science Letters* 298: 183–190.

Rosenfeld, C.L., and G.L. Beach. 1983. *Evolution of a drainage network—remote sensing analysis of the North Fork Toutle River, Mount St. Helens, Washington*, Water Resources Research Institute Report WRRI-88. Corvallis: Oregon State University Press.

Rowley, P.D., M.A. Kuntz, and N.S. MacLeod. 1981. Pyroclastic-flow deposits. In *The 1980 eruptions of Mount St. Helens, Washington*, Professional Paper 1250, ed. P.W. Lipman and D.R. Mullineaux, 489–512. Washington, DC: U.S. Geological Survey.

Sarna-Wojcicki, A.M., S. Shipley, R.B. Waitt Jr., D. Dzurisin, and S.H. Wood. 1981. Areal distribution, thickness, mass, volume, and grain size of air-fall ash from the six major eruptions of 1980. In *The 1980 eruptions of Mount St. Helens, Washington*, Professional Paper 1250, ed. P.W. Lipman and D.R. Mullineaux, 577–600. Washington, DC: U.S. Geological Survey.

Schuster, R.L. 1981. Effects of the eruptions on civil works and operations in the Pacific Northwest. In *The 1980 eruptions of Mount St. Helens, Washington*, Professional Paper 1250, ed. P.W. Lipman and D.R. Mullineaux, 701–718. Washington, DC: U.S. Geological Survey.

Scott, K.M. 1988. *Origins, behavior, and sedimentology of lahars and lahar-runout flows in the Toutle-Cowlitz River system*, Professional Paper 1447-A. Washington, DC: U.S. Geological Survey.

Sigurdsson, H., S.N. Carey, and J.M. Epindola. 1984. The 1982 eruptions of El Chichón Volcano, Mexico: Stratigraphy of pyroclastic deposits. *Journal of Volcanology and Geothermal Research* 23: 11–37.

Sigurdsson, H., B. Houghton, S. McNutt, H. Rymer, and J. Stix, eds. 2015. The encyclopedia of volanoes, 2nd edition. Amsterdam: Academic Press.

Simon, A. 1992. Energy, time, and channel evolution in catastrophically disturbed fluvial systems. *Geomorphology* 5: 345–372.

———. 1999. *Channel and drainage-basin response of the Toutle River system in the aftermath of the 1980 eruption of Mount St.*

Helens, Washington, Open-File Report 96–633. Washington, DC: U.S. Geological Survey.

Simon, A., and C.R. Thorne. 1996. Channel adjustment of an unstable coarse-grained stream: Opposing trends of boundary and critical shear stress, and the applicability of extremal hypotheses. *Earth Surface Processes and Landforms* 21: 155–180.

Surono, P. Jousset, J. Pallister, M. Boichu, M.F. Buogiorno, A. Budisantoso, F. Costa, S. Andreasuti, F. Prata, D. Schneider, L. Clarisse, H. Humaida, S. Sumarti, C. Bignami, J. Griswold, S. Carn, C. Oppenheimer, and F. Lavigne. 2012. The 2010 explosive eruption of Java's Merapi volcano—A '100-year' event. *Journal of Volcanology and Geothermal Research* 241-242: 121–135.

Swanson, F.J., and J.J. Major. 2005. Physical events, environments, and geological-ecological interactions at Mount St. Helens—March 1980–2004. In *Ecological Responses to the 1980 Eruption of Mount St. Helens*, ed. V.H. Dale, F.J. Swanson, and C.M. Crisafulli, 27–44. New York: Springer.

Swanson, F.J., B.D. Collins, T. Dunne, and B.P. Wicherski. 1983. Erosion of tephra from hillslopes near Mount St. Helens and other volcanoes. In *Proceedings of symposium on erosion control in volcanic areas*, Public Works Research Institute Technical Memorandum 1908, 183–221. Tsukuba: Ministry of Construction.

Townsend, J.R. 2013. The development of a geomatics-based toolkit to assess the impact of engineered grade building structures on the North Fork Toutle River, Mt. St. Helens. MS thesis. Nottingham: University of Nottingham.

Voight, B. 1981. Time scale for the first moments of the May 18 eruption. In *The 1980 eruptions of Mount St. Helens, Washington*, Professional Paper 1250, ed. P.W. Lipman and D.R. Mullineaux, 69–86. Washington, DC: U.S. Geological Survey.

Voight, B., H. Glicken, R.J. Janda, and P.M. Douglass. 1981. Catastrophic rockslide avalanche of May 18. In *The 1980 eruptions of Mount St. Helens, Washington*, Professional Paper 1250, ed. P.W. Lipman and D.R. Mullineaux, 347–377. Washington, DC: U.S. Geological Survey.

Waitt, R.B. 1981. Devastating pyroclastic density flow and attendant air fall of May 18—stratigraphy and sedimentology of deposits. In *The 1980 eruptions of Mount St. Helens, Washington*, Professional Paper 1250, ed. P.W. Lipman and D.R. Mullineaux, 439–460. Washington, DC: U.S. Geological Survey.

———. 1989. Swift snowmelt and floods (lahars) caused by great pyroclastic surge at Mount St. Helens volcano, Washington, 18 May 1980. *Bulletin of Volcanology* 52: 138–157.

———. 2015. *In the path of destruction—eyewitness chronicles of Mount St. Helens*. Pullman: Washington State University Press.

Waitt, R.B., T.C. Pierson, N.S. MacLeod, R.J. Janda, B. Voight, and R.T. Holcomb. 1983. Eruption-triggered avalanche, flood, and lahar at Mount St. Helens—Effects of winter snowpack. *Science* 221: 1394–1397.

Warrick, J.A., J.A. Bountry, A.E. East, C.S. Magirl, T.J. Randle, G. Gelfenbaum, A.C. Ritchie, G.R. Pess, V. Leung, and J.J. Duda. 2015. Large-scale dam removal on the Elwha River, Washington, USA: Source-to-sink sediment budget and synthesis. *Geomorphology* 246: 729–750.

West Consultants, Inc. 2002. Mount St Helens engineering reanalysis: Hydrologic, hydraulic, and sedimentation analysis. Technical report prepared for U.S. Army Corps of Engineers Portland District. Bellevue, WA: West Consultants.

Western Regional Climate Center. 2015. Historical climate information, western U.S. climate data summaries. www.wrcc.dri.edu/climatedata/comparative/. Last accessed 14 May 2015.

Wheaton, J.M., J. Brasington, S.E. Darby, and D.A. Sear. 2010. Accounting for uncertainty in DEMs from repeat topographic surveys: Improved sediment budgets. *Earth Surface Processes and Landforms* 35: 136–156.

White, J.D.L., B.F. Houghton, K.A. Hodgson, and C.J.N. Wilson. 1997. Delayed sedimentary response to the AD 1886 eruption of Tarawera, New Zealand. *Geology* 25: 459–462.

Wickert, A.D., J.M. Martin, M. Tal, W. Kim, B. Sheets, and C. Paola. 2013. River channel lateral mobility: Metrics, time scales, and controls. *Journal of Geophysical Research – Earth Surface* 118: 396–412. https://doi.org/10.1029/2012JF002386.

Wilcox, A.C., J.E. O'Connor, and J.J. Major. 2014. Rapid reservoir erosion, hyperconcentrated flow, and downstream deposition triggered by breaching of 38 m tall Condit Dam, White Salmon River, Washington. *Journal of Geophysical Research – Earth Surface* 119: 1376–1394.

Willingham, W.F. 2005. The Army Corps of Engineers' short-term response to the eruption of Mount St. Helens. *Oregon Historical Quarterly* 106 (2): 174–203.

Winner, W.E., and T.J. Casadevall. 1981. Fir leaves as thermometers during the May 18 eruption. In *The 1980 eruptions of Mount St. Helens, Washington*, Professional Paper 1250, ed. P.W. Lipman and D.R. Mullineaux, 315–320. Washington, DC: U.S. Geological Survey.

Wohl, E. 2000. *Mountain rivers*, Water Resources Monograph 14. Washington, DC: American Geophysical Union.

Yamakoshi, T., Y. Doi, and N. Osanai. 2005. Post-eruption hydrology and sediment discharge at the Miyakejima volcano, Japan. *Zeitschrift für Geomorphologie Supplement Band* 140: 55–72.

Zehfuss, P.H., B.F. Atwater, J.W. Vallance, H. Brenniman, and T.A. Brown. 2003. Holocene lahars and their by-products along the historical path of the White River between Mount Rainier and Seattle. In *Western cordilleran and adjacent areas*, Field Guide 4, ed. T.W. Swanson, 209–223. Boulder: Geological Society of America.

Zheng, S., B. Wu, C. Thorne, and A. Simon. 2014. Morphological evolution of the North Fork Toutle River following the eruption of Mount St. Helens, Washington. *Geomorphology* 208: 102–116.